R64

FISCAL YEAR 199
YEAR-END REPOR

For the November 1997 to October 1998 Peri

PLUGGING AND UNPLUGGING OF WASTE TRANSFER PIPELINES

Preliminary Data and Results

Principal Investigator:

M.A. Ebadian, Ph.D.

Florida International University
Collaborators:

C.X. Lin, Ph.D.
J.L. Xu, Ph.D.

Prepared for:

U.S. Department of Energy
Office of Environmental Management
Office of Science and Technology

HEMISPHERIC CENTER FOR ENVIRONMENTAL TECHNOLOGY (HCET)
Florida International University, Center for Engineering & Applied Sciences

DISCLAIMER

PLUGGING AND UNPLUGGING OF WASTE TRANSFER PIPELINES

Principal Investigator

M.A. Ebadian, Ph.D.
Hemispheric Center for Environmental Technology
Florida International University
Miami, FL 33174

Florida International University Collaborators

C.X. Lin, Ph.D.
J.L. Xu, Ph.D.
Hemispheric Center for Environmental Technology
Florida International University
Miami, FL 33174

January 1999

Prepared for

U.S. Department of Energy
Office of Environmental Management
Office of Science and Technology

Under Grant No.: DE-FG21-95EW55094

ACKNOWLEDGMENTS

The results presented in the present report were obtained from the work supported by the U.S. Department of Energy (DOE), Environmental Management (EM), Office of Science and Technology (OST) under Grant No. DE-FG21-95EW55094. The Principal Investigator and the associate researchers at the Hemispheric Center for Environmental Technology would like to thank Peter W. Gibbons, manager of Retrieval Technology Integration, DOE Tanks Focus Area, Numatec Hanford Corporation (NHC), for his guidance and suggestions. The authors are also grateful for the useful discussions with Dr. Fadel F. Erian at Pacific Northwest National Laboratory (PNNL). We would especially like to thank the DOE-OST for their support and encouragement throughout this research.

TABLE OF CONTENTS

ACRONYMS iv
LIST OF FIGURES v
LIST OF TABLES vi
EXECUTIVE SUMMARY vii
1.0 INTRODUCTION 1
2.0 EXPERIMENTAL SETUP 3
2.1 Test Section 3
2.2 Parameter Measurement and Uncertainty Analysis 3
2.3 Data Acquisition System 4
2.4 Experimental Loop Collaboration 4
3.0 SLURRY SIMULANTS AND THEIR PROPERTIES 7
3.1 Density 9
3.2 Volume Concentration 9
3.3 Viscosity 10
4.0 FLOW CHARACTERISTICS FOR TYPICAL SLURRY SIMULANTS IN HORIZONTAL PIPES 19
4.1 Volume Concentration Effect 20
4.2 Particle Size Effect 20
4.3 Pressure Gradient Correlation 20
5.0 FLOW PATTERN AND WEIGHT CONCENTRATION DISTRIBUTION ALONG FLOW DIRECTION 28
5.1 Pseudo-homogeneous flow 28
5.2 Heterogeneous flow 28
5.3 Stationary bed flow 28
5.4 Moving bed flow 29
6.0 RESUSPENSION TRANSITION FOR SLURRY FLOWING IN HORIZONTAL PIPES 32
7.0 THE DESIGN OF PIPELINE PLUGGING AND UNPLUGGING LARGE-SCALE DEMONSTRATION TEST BED 36
8.0 MAJOR ACCOMPLISHMENTS AND CONCLUSIONS 41
9.0 PLANNED ACTIVITIES FOR FY99 42
10.0 REFERENCES 45

ACRONYMS

DOE	U.S. Department of Energy
EM	Environmental Management
FETC	Federal Energy Technology Center
FIU	Florida International University
FY98	Fiscal Year 1998
FY99	Fiscal Year 1999
HCET	Hemispheric Center for Environmental Technology
HLW	High-Level Waste
NHC	Numatec Hanford Corporation
OST	Office of Science and Technology
PNNL	Pacific Northwest National Laboratory
SRS	Savannah River Site
TFA	Tanks Focus Area

LIST OF FIGURES

Figure 1. Test loop and the main parameter measurement. 5
Figure 2. The plugging & unplugging flow loop experimental loop. 5
Figure 3. Comparison of measured friction factor with calculated values. 6
Figure 4. Shear stress versus shear rate for typical non-Newtonian fluids. 16
Figure 5. Shear stress versus shear rate for slurry A and slurry B (concentration effect). 16
Figure 6. Shear stress versus shear rate for slurry B and slurry C (particle size effect). 17
Figure 7. Shear stress versus shear rate for slurry D and slurry E (particle size effect). 17
Figure 8. Shear stress versus shear rate for slurry E and slurry F (concentration effect). 18
Figure 9. Typical wall shear stress versus shear rate for simple slurry. 23
Figure 10. Wall shear stress versus shear rate for the six slurry simulants. 24
Figure 11. Pressure gradient versus flow velocity (volume concentration effect). 25
Figure 12. Pressure gradient versus flow velocity (particle size effect). 25
Figure 13. Pressure gradient versus flow velocity (particle size effect). 26
Figure 14. Pressure gradient versus flow velocity (volume concentration effect). 26
Figure 15. Friction factor versus flow velocity 27
Figure 16. Over-pressure term versus modified Fr number and comparison with the classical correlation. 27
Figure 17. Weight concentration for slurry C along axial distance (case 1) 30
Figure 18. Weight concentration for slurry C along axial distance (case 2) 30
Figure 19. Weight concentration for slurry C along axial distance (case 3) 31
Figure 20. Pressure gradient versus time for resuspension transition with slurry A. 34
Figure 21. Flow velocity versus time for resuspension transition for slurry A. 35
Figure 23. Pipeline plugging and unplugging large scale demonstration test bed- simulated case #1. 37
Figure 24. Pipeline plugging and unplugging large scale demonstration test bed- simulated case #2. 38
Figure 25. Pipeline plugging and unplugging large scale demonstration test bed- simulated case #3. 39
Figure 26. Pipeline plugging and unplugging large scale demonstration test bed- simulated case #5. 40

LIST OF TABLES

Table 1. Results on optimal SRS sludge sample #32897, data on bottle: Oct.10, 19,1995 7
Table 2. Results on optimal Hanford slurry sample 8
Table 2a. Major slurry simulant properties 9
Table 3. Physical properties of slurry A (10% wt SRS slurry with "fine" particles) 11
Table 4. Physical properties of slurry B (20% wt SRS slurry with "fine" particles) 12
Table 5. Physical properties of slurry C (20% wt SRS slurry with "coarse" particle size of 180~250 μm) 13
Table 6. Physical properties of slurry D (20% wt Hanford slurry with "coarse" particle size of 180~250 μm) 14
Table 7. Physical properties of slurry F (30% wt Hanford slurry with "coarse" particle size of 250~500 μm) 15
Table 8. Critical velocities of the six slurry simulants 20
Table 9. Weight concentration run-case parameter 29
Table 10. The resuspension velocity for the six slurry simulants 33
Table 11. The maximum pressure gradient for the unplugging of the horizontal pipe 33

EXECUTIVE SUMMARY

The plugging and unplugging of waste transfer pipelines conducted by Florida International University's Hemispheric Center for Environmental Technology (FIU-HCET) for the year 1998 (FY98) is summarized in this report. The objective is to determine optimal mixing, settling, pipe plugging and unplugging of the waste slurry transfer pipeline system for High-Level Waste (HLW). The investigation focuses on recreating pipeline plugging conditions for equipment testing of plug locating and removal and providing systematic operating data for modification of equipment design and enhancement of performance of the waste slurry transfer lines used at DOE sites.

The project consists of two parts. The first part, which is the major work performed this year, is the flow loop investigation of the mixing, settling, and pipe plugging and unplugging of waste transfer lines. The second part is the Large-Scale Plug Locating and Removal Demonstration Test Bed for an industrial equipment test and demonstration. FIU-HCET finished the test bed concept design in FY98.

A test loop for slurry flowing in horizontal pipe or pipe with a dip has been constructed in the FIU-HCET laboratory. The loop consists of the mixing tank, pump, pipelines, and corresponding measurement transducers. An efficient sampling system was developed in the flow loop. The system extracts the samples from the top and bottom points along the flow distance. The LabView Data Acquisition System was applied to record and store the steady or transition data. Six typical slurry simulants of interest to DOE sites were used. Among them three simulated Savannah River slurries and three Hanford slurries. The physical properties of the slurry simulants were measured or calculated, including density, volume concentration, particle size and viscosity, and so on. The viscosity was measured by the HAKKE viscometer.

Preliminary experimental data and results on the typical slurry simulants flowing in horizontal pipes were provided, and the main results are in this report. The study paid much attention to the flow characteristics, settling, and pipeline plugging and unplugging. Both the decreasing flow and increasing flow tests were performed. The tests did not cover high-flow velocity due to the limits of the slurry pump capacity. The type of pump does not change, but a pump with high flow rate is being prepared to install in the flow loop, so that the data will be more useful for engineering proposes.

The present slurry simulants did show the distinct flow characteristics found in existing research on the simple slurries. With the present parameter ranges, the flow has two main flow patterns: heterogeneous flow and stationary bed flow. The transition from the heterogeneous flow to the stationary bed flow appeared on the critical velocity, which is important for the pipeline design in order to avoid particle settling. Higher particle volume concentration will result in a higher critical velocity. With the heterogeneous flow pattern, the weight concentration measurements from the top point and bottom point show that there is always concentration gradient across the vertical coordinate, but no gradient exists along the flow direction. The concentration gradient also decreases with increasing flow velocity.

With stationary bed flow, further decreasing the velocity will result in more and more particle settling. The available flow area is decreased, and eventually the pipe is plugged. When this occurs, the flow meter shows zero velocity, even though the pump is operating.

A correlation was recommended to predict the pressure gradient (flow resistance). The resuspension tests were also done to unplug the horizontal pipe. It was found that two typical periods, which have different characteristics, existed during the whole unplugging process. The maximum pressure gradients (unplugging resistance) and the suspension velocities for the typical slurry simulants were obtained. At the fixed particle volume concentration, the slurry simulants with fine particles will get higher unplugging resistance. At the fixed particle sizes, the larger volume concentration will get higher unplugging resistance.

The concept design of the large-scale test bed for the plugging and unplugging demonstration has been finished. The original five cases provided in the document "Functions and Requirements for Blockage Locating and Removal Methods in Waste Transfer Lines" were condensed to three cases. Each simulated case represented some aspects of the original cases. The design contained both buried pipe and unburied pipes. The detailed design of the test bed is in process.

As a continuation of FY98's research, the gelling-caused plugging and unplugging will be the major research work in FY99 using the same flow loop used in FY98. In addition to this, a test bed will be designed and constructed at FIU-HCET for the industrial equipment test and demonstration. Based on the previous study of pipeline plugging, credible blockage will be prepared in the test bed for the equipment test and demonstration. A monitoring system to ensure the pipeline is really unplugged will be developed. Tests will be conducted for both buried pipe and unburied pipes.

1.0 INTRODUCTION

This project, which began in FY97, involves both the flow loop research on plugging and unplugging of waste transfer pipelines, and the large-scale industrial equipment test of plugging locating and unplugging technologies. In FY98, the related work was performed under the project name "Mixing, Settling, and Pipe Unplugging of Waste Transfer Lines." The mixing, settling, and pipeline plugging and unplugging are critical to the design and maintenance of a waste transfer pipeline system, especially for the High-Level Waste (HLW) pipeline transfer. The major objective of this work is to recreate pipeline plugging conditions for equipment testing of plug locating and removal and to provide systematic operating data for modification of equipment design and enhancement of performance of waste transfer lines used at DOE sites.

As the waste tank clean-out and decommissioning program becomes active at the DOE sites, there is an increasing potential that the waste slurry transfer lines will become plugged and unable to transport waste slurry from one tank to another or from the mixing tank to processing facilities. Transfer systems may potentially become plugged if the solids concentration of the material being transferred increases beyond the capability of the prime mover or if upstream mixing is inadequately performed. Plugging can occur due to the solids' settling in either the mixing tank, the pumping system, or the transfer lines. In order to enhance and optimize the slurry's removal and transfer, refined and reliable data on the mixing, sampling, and pipe unplugging systems must be obtained based on both laboratory-scale and simulated in-situ operating conditions.

Many operating parameters, such as solids concentration, solid particle size, chemical nature of the solids, slurry pH value, pipeline geometry, pipeline distance, pumping speed, and operating temperature, can affect the slurry settling and pipe-plugging characteristics in the slurry transfer systems. Among them the solid volume concentration, particle density, and particle size are the three key parameters to affect the particle settling and slurry flow. To obtain systematic and optimal data on the waste slurry flows transfer lines, both experimental and theoretical methods were used in this study. The sampling systems were also developed to monitor the settling and pipe-plugging progress. Investigation of the settling and pipe-plugging behaviors in a pipeline system has been emphasized. All the experimental and numerical data have been correlated to provide formulations for engineering applications.

A literature survey showed that available references concentrated on simple slurry, such as water-sand, coal-water, two-phase flow in horizontal pipes. Generally, the flow covered high velocity. Little information can be obtained on low flow velocity. The authors believe this is because it is difficult to get pressure drop information at low flow velocity. However, it is important to know how the particle bed is forming at low flow velocity. Despite best efforts, no study on the gelling-caused plugging could be found.

The major work performed in FY98 focused on the flow loop research on the pipeline plugging and unplugging of typical slurry simulants of interest to DOE sites. A flow loop, which contains the mixing tank, pump, horizontal pipe or the pipes with a dip and the corresponding measurement transducers, was established. A reliable sampling system was also developed to analyze the concentration versus the vertical cross-section and the flow distance. Both the decreasing flow and increasing flow test were conducted. Some important data, which are key to the design and maintenance of the waste transfer lines, are obtained. These include 1) the critical

velocity, at which the solid particles settled in the bottom of the pipe; 2) the resuspension velocity, at which the solid particles resuspended; and 3) the maximum pressure gradient to overcome the flow resistance for the unplugging process.

A new slurry pump with high flow rate is being prepared for flow loop installation. The sampling system is also being modified in order to drain the samples more accurately.

The major purpose of the large-scale industrial equipment test of plug locating and unplugging is to identify suitable plug locating and unplugging technologies for HLW transfer pipelines at DOE sites. The selection of industrial companies and the technologies to be tested will be carried out in collaboration with NHC, PNNL, FETC, DOE, and DOE sites, including Hanford, Savannah River, and Oak Ridge. The test bed will be designed and constructed based on the "Functions and Requirements for Blockage Locating and Blockage Removal Methods in Waste Transfer Lines" issued by SRS in FY88. Based on the previous study of pipeline plugging, credible blockage will be prepared in the test bed for the equipment test and demonstration. Tests will be conducted primarily on unburied pipes. Buried pipes may be used in the test of certain technologies. Analysis and evaluation of the tested pipeline plug locating and unplugging technologies will be performed. A report recommending technologies to locate and unplug waste transfer pipeline plugs will be provided to DOE. The inspection tools will also be tested in the test bed.

The flow loop research on gelling-caused plugging and unplugging will also be carried out in FY99.

The experimental and theoretical results produced in FY98, when applied in the DWPF slurry transfer lines, can enhance and modify the technical base for designing slurry transportation equipment and pipeline systems. These results will also serve as an important reference for improving waste slurry mixing performance in waste processing facilities. Interested vendors and users will then be given the opportunity to demonstrate the effectiveness of their equipment in satisfying these specifications.

2.0 EXPERIMENTAL SETUP

To provide information on the plugging and unplugging of typical slurry simulants flowing in pipelines, an experimental loop was set up in the FIU-HCET laboratory. The loop consists of a mixing tank, pump, horizontal pipe, and corresponding measurement transducers. At the pump exit, the fluid travels through the flow-developing section, including a half-circular pipe, then flows through the main test section, and eventually back to the mixing tank. The half-circular section of the pipe is used to remove the effect of the secondary flow. Figure 1 shows the loop schematically. Figure 2 is a picture of the loop. In the mixing tank, a mixer powered by an electric motor was installed to agitate the slurry mixture to get a homogeneous concentration distribution in the tank. The rotating speed is shown on a speed rotameter. A water tank and a collection tank were set up for use in loop cleaning.

2.1 TEST SECTION

The main test section is a long horizontal pipe with an outside diameter of 1.0 inch (25.4 mm). The corresponding inner diameter of the pipe is 0.87 inch (22.1 mm). The pipe length is 43 ft, so the pipe length to pipe diameter ratio L/D is 592.

In order to observe the particle settling process, two visual sections made of plastic tube, one at the entrance and the other at the exit of the main test section, were installed. The inside diameter of the visual section tube is the same as that of the main test section, so the plastic tube visual section can be connected to the horizontal test section smoothly using fittings. During loop operation, pictures identifying the flow pattern can be taken through the visual sections.

Eight sampling tubes with outside diameters of one-quarter inch are arranged along the main test section. Among these sampling tubes, four are arranged at the top of the pipe and marked as "1, 3, 5, and 7." Another four are at the bottom of the pipe marked as "2, 4, 6, and 8." Each sampling tube consists of a gate valve. By opening the gate valve, slurry samples can be taken from the main horizontal pipe. During the slurry sampling process, the ratio of the sampling tube flow rate to the horizontal pipe flow rate can be kept nearly constant by adjusting the valve opening . The locations of these tubes are shown on Figure 1.

At present, the sampling tubes are vertical to the main flow direction, thus, affecting the flow field when the slurry is drained through them. A new and more effective sampling tube system is in development.

2.2 PARAMETER MEASUREMENT AND UNCERTAINTY ANALYSIS

Two pressure transducers and three differential pressure transducers are installed in the loop. The first and third differential pressure transducer is placed across a pipe length of 19.5 ft. The second differential pressure transducer is placed across a pipe length of 2.0 ft. All the differential pressure transducers had the range of 150-inch water. The flow rate can be adjusted by the pump rotating speed, and was measured by the electromagnetic volume flow meter. The range of the electromagnetic volume flow meter could be adjusted manually based on the experimental needs. The pressure transducers and the differential transducers have a high measuring accuracy of 0.25%. The uncertainty of the volume flow rate is estimated to be 1.0%.

The operating parameters are

differential pressure	50 inch water (across 19.5 ft length)
velocity	0.1~1.5 m/s

2.3 DATA ACQUISITION SYSTEM

The LabVIEW Data Acquisition System records the data and saves it to disk for further analysis.

2.4 EXPERIMENTAL LOOP CALIBRATION

In order to verify the applicability of the loop, clear water was used as the working fluid to first calibrate the loop. Figure 3 presented the calibration result, in which the measured friction factor and the classical values were shown. The friction factor was defined as

$$f = \frac{\Delta P}{L} \times \frac{2D}{\rho V^2} \tag{1}$$

where $\Delta P/L$ is the pressure gradient, D is the pipe inside diameter, ρ is the liquid density, and V is the flow velocity.

In the fully turbulent region, the friction factor is well correlated as $f=0.3164/Re^{0.25}$ for smooth pipe. Figure 3 shows that the two curves agree with each other very well; the maximum error is less than 2.0%.

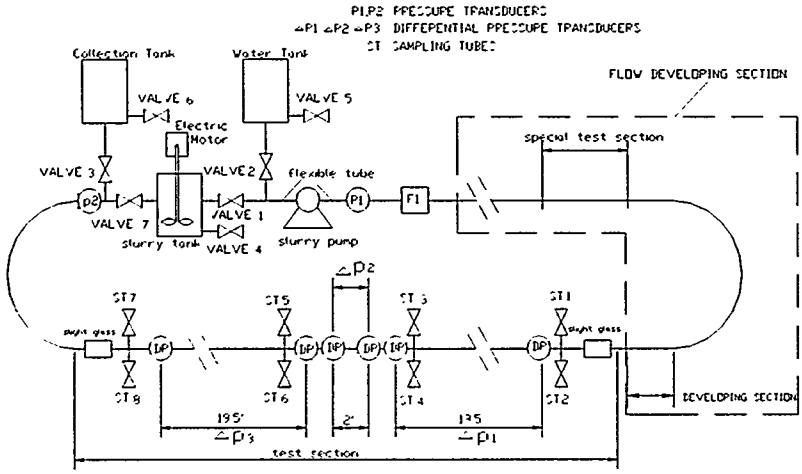

Figure 1.Test loop and the main parameter measurement.

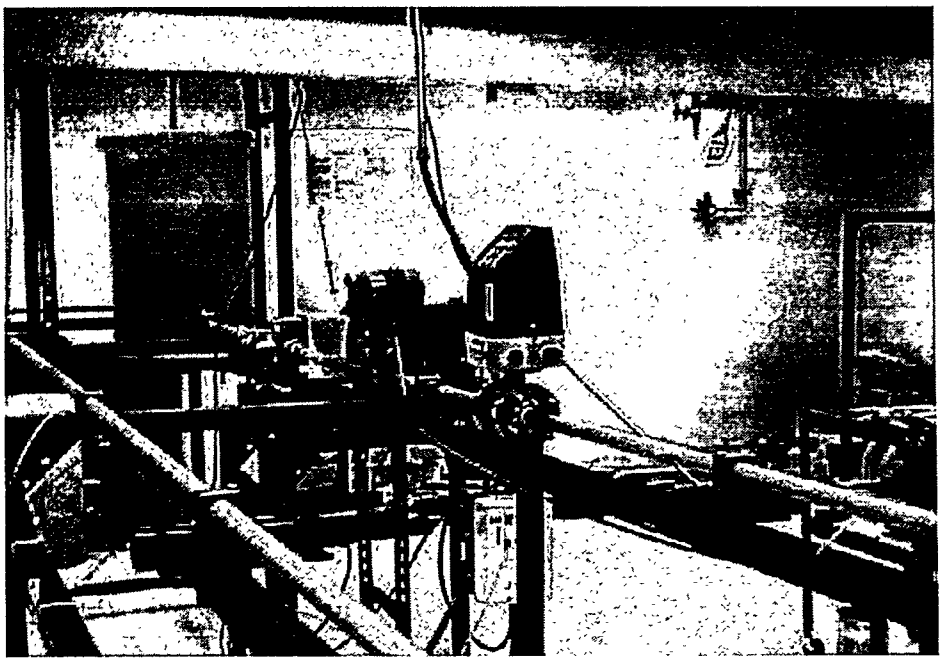

Figure 2. The plugging & unplugging flow loop experimental loop.

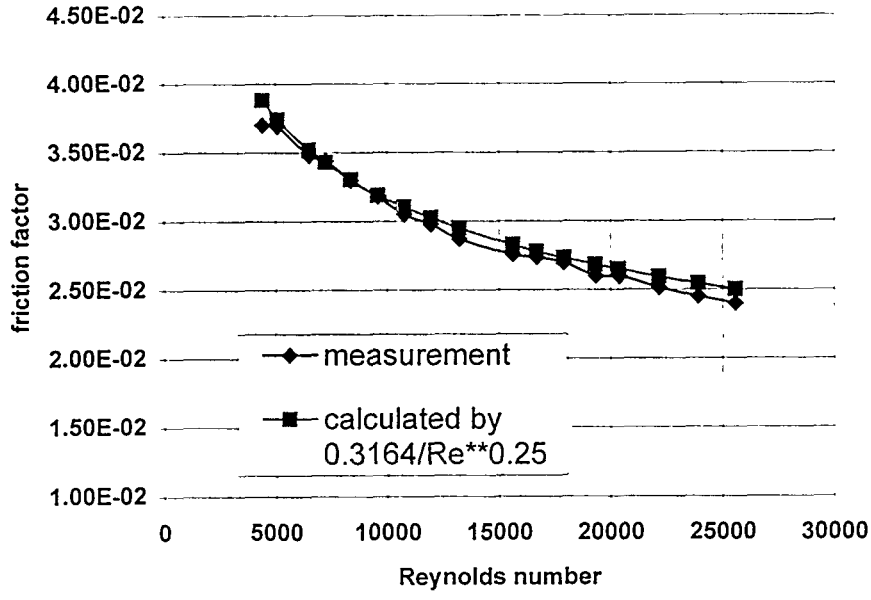

Figure 3. Comparison of measured friction factor with calculated values.

3.0 SLURRY SIMULANTS AND THEIR PROPERTIES

Six typical slurry simulants of interest to DOE sites were used in this investigation. The proposed slurry simulants included both Savannah River slurry simulants and Hanford slurry simulants.

Generally there are five parameters affecting the flow characteristics of the slurry in pipelines: carry fluid viscosity, density ratio, volume concentration, particle size, and particle size distribution. In order to get information on the plugging and unplugging characteristics for typical slurry simulants close to the situations at DOE sites, six slurry simulants were tested. The weight concentration covered the range from 10 to 30%, and the particle size had the range from 5 to 500μm. The slurry simulants were prepared based on data of results on an optimal sample, neglecting some very small weight concentration components. Table 1 and Table 2 summarize the typical results on an optimal sludge sample.

Table 1.
Results on optimal SRS sludge sample #32897, data on bottle: Oct.10, 19,1995

Major Components	Weight Concentration(wt %)
Al	6.76
Ca	2.67
Fe	26.8
Mg	1.31
Mn	2.80
Na	10.2
Si	0.81
CO_3	1.94
NO_3	1.96
NO_2	5.86
Total	61.11

The above components total a weight concentration of 61.11%. Therefore, water (or some similar liquid) covers 38.89%.

In preparing the slurry simulants in the laboratory, the oxide that contains the major component such as Al_2O_3, is used. The relative weight concentration of each major component is kept at the same value, as shown in Table 1. The insoluble oxide particle size and density were found in the chemical textbook. SiO_2, which was available in the laboratory, was used to simulate the solid particle density, particle sizes and size distribution. The SiO_2 solid particles were dried, selected, and measured in the laboratory.

Table 2 gives the major components of Hanford slurry simulants.

Table 2.
Results on optimal Hanford slurry sample

Major Components	Weight concentration, wt%
Ni	2.44
Mn	2.22
Fe	27.3
Al	6.3
Zr	14.2
Na	1.38
Total	53.84

Three SRS slurry simulants studied at FIU-HCET are

- 10% wt concentration, with water, Fe_2O_3, Al_2O_3, $CaCO_3$, MnO_2, NaOH, $NaNO_2$ and $Mg(NO_3)_2$ as the components, named as slurry A with "fine" particle size of 1.2~150 μm
- 20% wt concentration, with water, Fe_2O_3, Al_2O_3, $CaCO_3$, MnO_2, NaOH, $NaNO_2$, and $Mg(NO_3)_2$ as the components, named as slurry B with "fine" particle size of 1.2~150 μm
- 20% wt concentration, with water, Fe_2O_3, Al_2O_3, $CaCO_3$, MnO_2, NaOH, $NaNO_2$, $Mg(NO_3)_2$, and SiO_2 with particle size of 180~250 μm as the components, named as slurry C.

The Hanford slurry simulants used in the present study are:

- 20% wt concentration, with water, Fe_2O_3, Al_2O_3, MnO_2, ZrO_2, Ni, and SiO_2 with particle size of 180~250 μm as the components, named as slurry D
- 20% wt concentration, with water, Fe_2O_3, Al_2O_3, MnO_2, ZrO_2, Ni, and SiO_2 with particle size of 250~500 μm as the components, named as slurry E
- 30% wt concentration, with water and Fe_2O_3, Al_2O_3, MnO_2, ZrO_2, Ni, and SiO_2 with particle size of 250~500 μm as the components, named as slurry F.

The six slurry simulants are summarized in the following table.

Table 2a.
Major slurry simulant properties

	Slurry A	Slurry B	Slurry C	Slurry D	Slurry E	Slurry F
Weight concentration	10%	20%	20%	20%	20%	30%
Volume concentration	2.54%	7.06%	7.06%	6.90%	6.90%	10.96%
Particle size (μm)	1.2~150	1.2~150	180~250	180~250	250~500	250~500
D_{50} (μm)			215	215	375	375

Through comparison of the results between slurry A and slurry B, one can identify how the concentration affects the flow. From the results of slurry B and slurry C, one can see how the particle size affects the flow. The three Hanford slurry simulants were chosen based on similar ideas. For each slurry, the pH value was controlled to be nearly 13 by adding a small quantity of NaOH to the slurry mixture. The pH value was recorded by the electric pH meter during the slurry-making process.

3.1 DENSITY

Theoretically, for the present slurry simulants, which consisted of water, SiO_2, and several insoluble particle components, the mixture density can be calculated as

$$\rho = \frac{1}{\sum \frac{C_{w,i}}{\rho_i}} \tag{2}$$

where $C_{w,i}$ means the weight concentration of i component, and ρ_i is the density of i component. The subscript i represents each component chemical in the slurry mixture. In equation (2), the unit of density is g/cm^3.

By weighing the net sample weight at a given volume, one can easily measure the density, as the net weight divided by the given volume. Two methods were developed; predicted densities are very close to the measured values. The results are summarized in Tables 3~7.

3.2 VOLUME CONCENTRATION

Volume concentration is one of the most important parameters affecting slurry flow. The volume concentration of j th component can be calculated based on the following equation:

$$C_{v,j} = C_{w,j} \frac{\rho_{mixture}}{\rho_j} \tag{3}$$

Therefore, the total volume concentration of all insoluble components is

$$C_v = \sum C_{w,j} \frac{\rho_{mixture}}{\rho_j} \tag{4}$$

where the subscript j represents each insoluble chemical component.

3.3 VISCOSITY

Viscosity is very useful for correlation of the pressure gradient, analyzing the critical velocity and the flow in the low velocity region. Figure 4 shows schematically the shear stress versus the shear rate for all kinds of fluids encountered in nature. Curve number one is typical of the response of a slurry that exhibits a yield stress, a so-called Bingham plastic. A Bingham plastic is characterized by a flow curve that is a straight line having an intercept τ_0 on the shear stress axis. The yield stress τ_0 is a measure of the stress that must be exceeded for flow to commence. The flow behavior is described by the equation:

$$\tau - \tau_o = \eta \frac{dV}{dy} \tag{5}$$

Curve number two shows a typical pseudoplastic fluid. This fluid does not exhibit a yield stress and has a flow curve whose slope decreases with an increasing rate of shear strain, until at high shear rates a limiting slope is reached. The rheology of pseudoplastic can be described by a number of models, the most commonly used being the Power Law model:

$$\tau = K\left(\frac{dV}{dy}\right)^n \quad \text{for } n<1.0 \tag{6}$$

Curve three shown in Figure 4 is a typical flow curve for so-called dilatant fluids. This type of fluid can also be described by the Power Law model, but with a flow index n>1.0. Curve four shown in the figure is a typical flow curve for pseudoplastic material having a yield stress.

The six slurry curves are illustrated in Figures 5~8. From these figures,

- Slurry B and slurry F showed the yield stress. No apparent yield stress existed for slurry A, C, D, and E. The flow characteristics of the slurry were quite complicated and affected by the combined effect of solid concentration, particle size, and chemical components.
- When shear rate was fixed, higher volume concentration got a higher shear stress (see Figure 5, curve of slurry A and slurry B, and Figure 8, curve of slurry E and slurry F).
- When volume concentration is fixed, slurry with "fine" particles gets higher shear stress (see Figure 6, curve of slurry B and slurry C). For slurry D and slurry E, particle size has little effect on the shear stress versus shear rate curve.
- Generally, for these present six slurry simulants, the shear stress versus shear rate curve tended to be the dilatant fluid, and the flow obtained little yield stress.

Because the present slurry simulants show little yield stress and can be treated as the dilatant fluids, the Power Law model was applied to correlate the data. The results are listed as follows:

$$\tau = 5.639\times10^{-4}\gamma^{1.4424} \quad \text{for slurry A}$$
$$\tau = 3.752\times10^{-3}\gamma^{1.1844} \quad \text{for slurry B}$$
$$\tau = 2.412\times10^{-4}\gamma^{1.5769} \quad \text{for slurry C}$$
$$\tau = 1.9903\times10^{-4}\gamma^{1.5832} \quad \text{for slurry D \& E}$$
$$\tau = 8.623\times10^{-4}\gamma^{1.4062} \quad \text{for slurry F}$$

Table 3.
Physical properties of slurry A (10% wt SRS slurry with "fine" particles)

Weight Concentration of the Slurry	10%
Volume Concentration of the Slurry	2.54%
Density of the Slurry	1.09 g/cm^3
Quantity of Water	63.52 kg(86.43% wt)
Quantity of Fe_2O_3	5.37 kg(7.3% wt)
Density of Fe_2O_3	5.24 g/cm^3
Size of Fe_2O_3	5 μm
Quantity of Al_2O_3	1.79 kg(2.44%)
Density of Al_2O_3	3.97 g/cm^3
Size of Al_2O_3	45~150 μm
Quantity of $CaCO_3$	0.467 kg(0.64%)
Density of $CaCO_3$	2.70 g/cm^3
Size of $CaCO_3$	1.2 μm
Quantity of MnO_2	0.31 kg(0.42%)
Density of MnO_2	5.026 g/cm^3
Size of MnO_2	Less than 45 μm
Carry Fluid Density	1.09 g/cm^3
Carry Fluid Viscosity	1112×10^{-6} kg/ms
Volume Concentration of Fine Particles in Carry Fluid C_f	2.54%

Table 4.
Physical properties of slurry B (20% wt SRS slurry with "fine" particles)

Weight Concentration of the Slurry	20%
Volume Concentration of the Slurry	7.06%
Density of the Slurry	1.19 g/cm^3
Quantity of Water	63.52 kg(78.01% wt)
Quantity of Fe_2O_3	10.74 kg(13.2% wt)
Density of Fe_2O_3	5.24 g/cm^3
Size of Fe_2O_3	5 μm
Quantity of Al_2O_3	3.58 kg(4.4%)
Density of Al_2O_3	3.97 g/cm^3
Size of Al_2O_3	45~150 μm
Quantity of $CaCO_3$	0.934 kg(1.14%)
Density of $CaCO_3$	2.70 g/cm^3
Size of $CaCO_3$	1.2 μm
Quantity of MnO_2	0.62 kg(0.76%)
Density of MnO_2	5.026 g/cm^3
Size of MnO_2	Less than 45 μm
Carry Fluid Density	1.19 g/cm^3
Carry Fluid Viscosity	Measured by HAKKE viscometer
Volume Concentration of Fine Particles in Carry Fluid C_f	7.06%

Table 5.
Physical properties of slurry C (20% wt SRS slurry with "coarse" particle size of 180~250 μm)

Weight Concentration of the Slurry	20%
Volume Concentration of the Slurry	7.06%
Density of the Slurry	1.19 g/cm^3
Quantity of Water	63.52 kg(78.01% wt)
Quantity of Fe_2O_3	5.37 kg(6.6% wt)
Density of Fe_2O_3	5.24 g/cm^3
Size of Fe_2O_3	5 μm
Quantity of Al_2O_3	1.79 kg(2.2%)
Density of Al_2O_3	3.97 g/cm^3
Size of Al_2O_3	45~150 μm
Quantity of $CaCO_3$	0.467 kg(0.57%)
Density of $CaCO_3$	2.70 g/cm^3
Size of $CaCO_3$	1.2 μm
Quantity of MnO_2	0.31 kg(0.38%)
Density of MnO_2	5.026 g/cm^3
Size of MnO_2	Less than 45 μm
Quantity of SiO_2(treated as "coarse" particles)	7.946 kg(9.75%)
Density of SiO_2(treated as "coarse" particles)	2.65 g/cm^3
Size of SiO_2(treated as "coarse" particles)	180~250 μm
Carry Fluid Density	1.114 g/cm^3
Carry Fluid Viscosity	1112×10^{-6} kg/ms
Volume Concentration of Fine Particles in Carry Fluid C_f	2.71%
Volume Concentration of "coarse" Particles in Slurry C_s	4.35%

Table 6.
Physical properties of slurry D (20% wt Hanford slurry with "coarse" particle size of 180~250 μm)

Weight Concentration of the Slurry	20%
Volume Concentration of the Slurry	6.90%
Density of the Slurry	1.165 g/cm^3
Quantity of Water	60.0 kg(80.0% wt)
Quantity of Fe_2O_3	4.60kg(6.13% wt)
Density of Fe_2O_3	5.24 g/cm^3
Size of Fe_2O_3	5 μm
Quantity of Al_2O_3	1.4025 kg(1.87%)
Density of Al_2O_3	3.97 g/cm^3
Size of Al_2O_3	45~150 μm
Quantity of ZrO_2	1.145 kg(1.53%)
Density of ZrO_2	5.85 g/cm^3
Size of ZrO_2	1.2 μm
Quantity of MnO_2	0.207 kg(0.276%)
Density of MnO_2	5.026 g/cm^3
Size of MnO_2	Less than 45 μm
Quantity of Ni	0.1438 kg
Density of Ni	8.9 g/cm^3
Size of Ni	20 μm
Quantity of SiO_2(treated as "coarse" particles)	7.50 kg(10%)
Density of SiO_2(treated as "coarse" particles)	2.65 g/cm^3
Size of SiO_2(treated as "coarse" particles)	180~250 μm
Carry Fluid Density ρ_f	1.098 g/cm^3
Carry Fluid Viscosity μ_f	1070×10^{-6} kg/ms
Volume Concentration of Fine Particles in Carry Fluid C_f	2.414%
Volume Concentration of "coarse" Particles in Slurry C_s	4.4814%

Slurry E is the same as slurry D except that the slurry contains SiO_2 particles with particle size of 250~500 μm.

Table 7.
Physical properties of slurry F (30% wt Hanford slurry with "coarse" particle size of 250~500 μm)

Weight Concentration of the Slurry	30%
Volume Concentration of the Slurry	10.96%
Density of the Slurry	1.271 g/cm^3
Quantity of Water	60.0 kg(70.0% wt)
Quantity of Fe_2O_3	5.24 kg(6.11% wt)
Density of Fe_2O_3	5.24 g/cm^3
Size of Fe_2O_3	5 μm
Quantity of Al_2O_3	2.40 kg(2.80%)
Density of Al_2O_3	3.97 g/cm^3
Size of Al_2O_3	45~150 μm
Quantity of ZrO_2	1.96 kg(2.28%)
Density of ZrO_2	5.85 g/cm^3
Size of ZrO_2	1.2 μm
Quantity of MnO_2	0.35 kg(0.408%)
Density of MnO_2	5.026 g/cm^3
Size of MnO_2	Less than 45 μm
Quantity of Ni	0.246 kg(0.28% wt)
Density of Ni	8.9 g/cm^3
Size of Ni	20 μm
Quantity of SiO_2(treated as "coarse" particles)	12.84 kg(15.0%)
Density of SiO_2(treated as "coarse" particles)	2.65 g/cm^3
Size of SiO_2(treated as "coarse" particles)	250~500 μm
Carry Fluid Density ρ_f	1.164 g/cm^3
Carry Fluid Viscosity μ_f	1123×10^{-6} kg/ms
Volume Concentration of Fine Particles in Carry Fluid C_f	4.063%
Volume Concentration of "coarse" Particles in Slurry C_s	7.19%

* In slurry A, B, and C, the insoluble chemical components of NaOH, $NaNO_2$, $Mg(NO_3)_2$ are also contained. However, their weight concentrations are less than 2.0%.

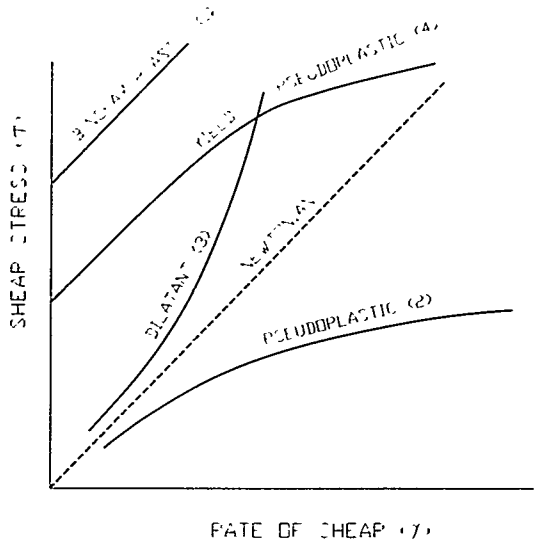

Figure 4. Shear stress versus shear rate for typical non-Newtonian fluids.

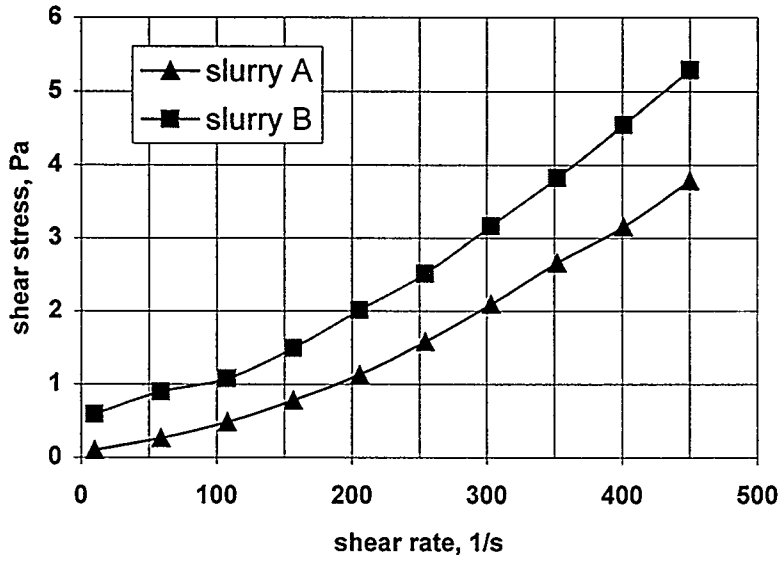

Figure 5. Shear stress versus shear rate for slurry A and slurry B (concentration effect).

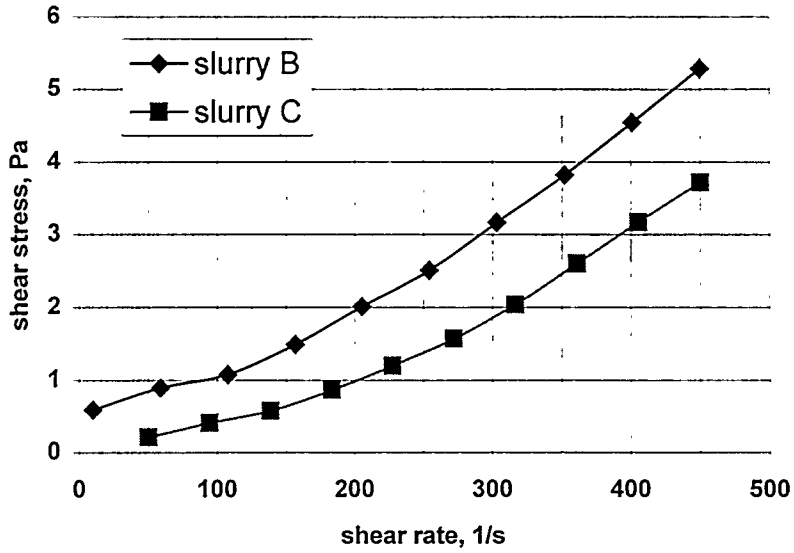

Figure 6. Shear stress versus shear rate for slurry B and slurry C (particle size effect).

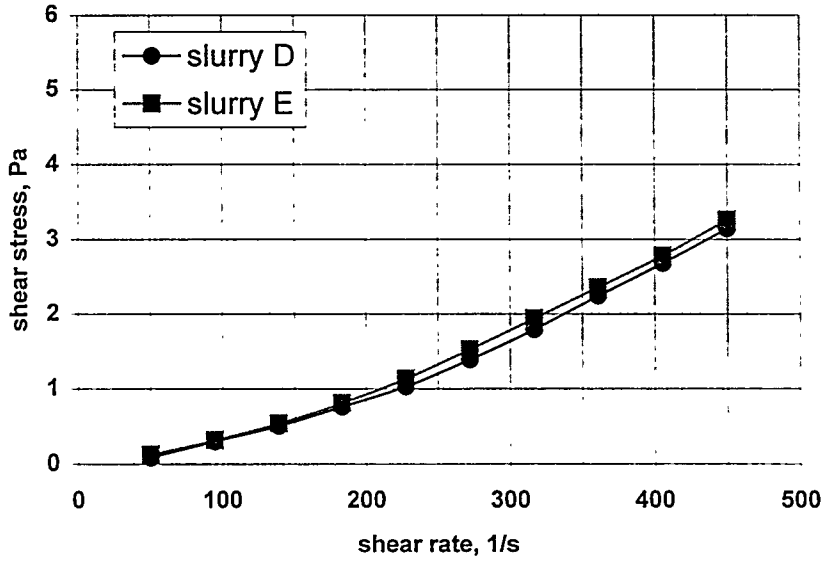

Figure 7. Shear stress versus shear rate for slurry D and slurry E (particle size effect).

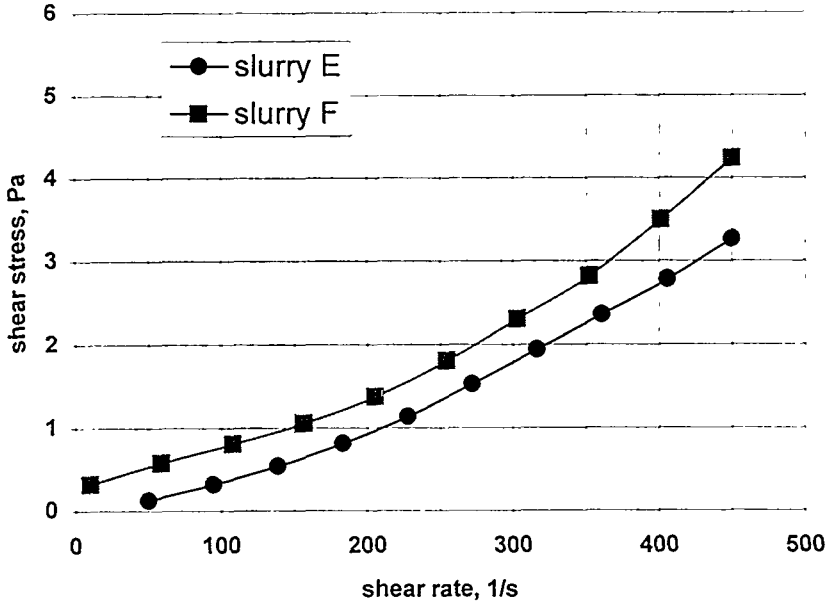

Figure 8. Shear stress versus shear rate for slurry E and slurry F (concentration effect).

4.0 FLOW CHARACTERISTICS FOR TYPICAL SLURRY SIMULANTS IN HORIZONTAL PIPES

Previous studies have concentrated on simple slurry, such as coal-water, flowing in horizontal pipes. For the coal-water, or sand-water system, literature, (e.g., E.J. Wasp 1978 presents the flow characteristics in horizontal pipelines. Figure 9 shows the typical response of classical slurry flowing in horizontal pipes. Generally, with velocity decrease, the flow changes to moving bed flow from the heterogeneous flow. Further decrease of the velocity will result in the stationary bed flow and eventually lead to the pipe plugging. In the moving bed flow region, the wall shear stress has a minimum value. The available literature names the corresponding velocity the critical deposition velocity. At velocity less than the critical deposition velocity, decreasing the velocity will result in the rise of the wall shear stress, followed by the stationary bed flow with nearly constant wall shear stress.

In the present study, decreasing the flow was accomplished by adjusting the pump rotating speed gradually until the new steady state was reached and the data was recorded by the Lab-View Data Acquisition System. The relationship between pressure drop ΔP and velocity V has been transferred to wall shear stress τ_w ($\frac{\Delta P}{L} \times \frac{D}{4}$) versus shear rate 8V/D; thus, the results can be used for other pipe diameters. Figure 10 illustrates the wall shear stress versus the shear rate for the six slurry simulants and clear water, in which the pressure drop ΔP that occurred in τ_w was from ΔP_1. This is because in decreasing flow test, ΔP_1 was always very close to ΔP_3. As shown in Figure 10, clear water showed the linear characteristics in the Log(τ_w)~Log(8V/D) curve.

Generally, for the six slurry simulants, at high velocity, the heterogeneous flow dominated in the pipe. This was verified by measuring the weight concentration distribution along the flow direction. The weight concentration was higher at the bottom than that at the top. The flow kept thesecharacteristics until the flow was decreased to a certain value, the critical velocity, at which the particles settled in the bottom of the pipe and stationary bed flow formed. The present report identifies this transition as the critical transition point.

For slurry A (10% wt with "fine" particles), the limit deposition transition point occurs at shear rate of 220 s^{-1}. This corresponds to the critical velocity of 0.61 m/s. Compared with other slurry simulants, slurry A has a lower critical velocity due to its lower volume concentration and the fine particles. Further decreasing the flow velocity from the critical velocity will result in a lower pressure gradient.

For slurry C, D, and E, the flow had the same characteristics. All the critical transition points appear at velocity of 0.83 m/s, corresponding to the shear rate of 300 s^{-1}. Generally, the chemical component differences among the three slurry simulants were not large. But slurry E has a particle size of 250~500 μm, larger than that of slurry D (180~250 μm). At lower velocity, the pressure gradient was larger for slurry D with smaller particle size than that for slurry E with larger particle size in the stationary bed flow. Decreasing the flow velocity from the critical velocity will result in a nearly constant pressure gradient, followed by the decreased pressure gradient region.

Slurry B (20% wt with "fine" particles) and slurry F (30% wt with particle size of 250~500 μm) had distinct flow characteristics compared with those for slurry A, C, D, and E. Slurry F had a

nearly constant pressure gradient in the whole stationary bed flow. While slurry B got an increased response with decreasing the flow velocity at the bed flow.

Table 8 shows the critical velocities for the six slurry simulants.

Table 8.
Critical velocities of the six slurry simulants

Slurry simulants	Critical Velocity (m/s)
A	0.61
C	0.83
D	0.84
E	0.83

The critical velocities for slurry B and slurry F are questionable due to the pump's capacity. Thus, the data were not listed in this report.

Figures 11~14 show the detailed pressure gradient versus the flow velocity, which identify the volume concentration effect and the particle size effect.

4.1 VOLUME CONCENTRATION EFFECT

Figure 11 shows the pressure gradient versus flow velocity with the same chemical components but with different volume concentrations. Higher volume concentration caused a higher pressure gradient. In stationary bed flow, slurry B with a higher concentration produced an increased response of the pressure gradient with decreasing flow velocity. However, decreased response was found with decreasing flow velocity for slurry A with a lower volume concentration. Similar effects were also found for slurry E and slurry F (see Figure 14). The volume concentration had strong effects on the flow characteristics.

4.2 PARTICLE SIZE EFFECT

As an unexpected result of the authors' test, increasing the particle size will decrease the pressure gradient when the flow velocity is fixed. Such phenomena indicate that the slurry solid-liquid flow is indeed a complex flow (see Figure 12 and Figure 13).

4.3 PRESSURE GRADIENT CORRELATION

It is difficult to determine the pressure gradient accurately, because the slurry has complicated chemical components and the particle size is non-uniform. The present work developed a correlation that will be described in detail below.

The present analysis was based on the idea that the slurry contains the carry fluid and the "coarse" particles. The carry fluid includes the fine particles with a size less than 74 μm. The "coarse" particles are particles with a size larger than 74 μm. The carry fluid properties were measured: the volume concentration, density, and viscosity. Results can be found in Tables 3~7.

Generally, both the particle density and the particle size affect the flow. In a real slurry system, it is difficult to find a solid chemical component with a density equal to the liquid. Thus, only solid particles whose sizes are very "fine" are incorporated to the carry fluid. This treatment is reasonable because, when the particle size is very fine, only a small velocity can make the particle suspend in the mixture, neglecting what the particle density is. This concept was also used by some other researchers (see Y.S. Fangary et al. 1997).

However, the carry fluid concept is confusing, even though the above description tries to clarify. In this report we use this concept to correlate the pressure gradient. Some other models will also be tried to correlate the pressure drop, and some comparisons will also be conducted.

The carry fluid viscosity can be modified to take the effect of fine particles into account as

$$\mu_f = \mu_l(1+2.5C_f+10.05C_f^2+0.00273\exp(16.6C_f)) \tag{7}$$

The above equation is widely used in slurry systems to calculate the carry fluid viscosity incorporating some very fine particles.

In the literature*(E.J. Wasp 1978)*, the pressure gradient data is correlated as

$$\frac{f_m - f_l}{f_l C_s}\text{(over-pressure term)}$$

versus

$$\frac{V^2}{gD}\frac{\rho_f}{\rho_s-\rho_f}\sqrt{C_D}\ \text{(modified Fr number).}$$

where

f_m=friction factor of slurry, $f_m = \dfrac{2\Delta PD}{L\rho_m V^2}$

$\Delta P/L$=measured pressure gradient

D=pipe diameter

V=velocity of the mixture

f_l=friction factor for carry fluid, $f_l = \dfrac{0.3164}{(VD\rho_f/\mu_f)^{0.25}}$

g=acceleration due to gravity

ρ_s=density of "coarse" particles

ρ_f=density of carry fluid

C_D="coarse" particle drag coefficient

Cs = volume concentration of coarse particle in slurry

The drag coefficient is a function of the particle Reynolds number based on the particle terminal velocity:

$$C_D = 0.44 \qquad \text{if } \mathrm{Re}=w_t d\rho_f/\mu_f > 1000 \tag{8}$$

$$C_D = \frac{24}{\mathrm{Re}}(1+0.15\mathrm{Re}^{0.687}) \quad \text{if } \mathrm{Re}<1000 \tag{9}$$

where d is the particle size and w_t, the terminal velocity, is

$$w_t = \left[\frac{4g(\rho_s-\rho_f)d}{3C_D\rho_f}\right]^{0.5} \tag{10}$$

Coupling Eq.8, Eq.9, and Eq.10, one can obtain C_D.

Figure 15 shows the friction factor versus velocity. Also shown in Figure 15 are the data for clear water. The friction factor almost keeps constant for clear water. However, at lower velocity, the friction factors for the four slurry simulants are much higher than that for clear water. This is reasonable because only part of the cross-section area of the pipe is available for the slurry flowing at low velocity. Figure 15 also shows that the friction factor is lower for larger particle size (slurry E) than for smaller particle size (slurry D).

Figure 16 illustrates the over-pressure term

$$\frac{f_m - f_l}{f_l C_s}$$

against

$$\mathrm{Fr}=\frac{V^2}{gD}\left(\frac{\rho_f}{\rho_s-\rho_f}\right)\sqrt{C_D}$$

for the slurry C, D, E, and F. Figure 16 also shows the classical over-pressure term correlation (see *E.J. Wasp 1978*).

$$\frac{f_m - f_l}{f_l C_s} = 82\left[\left(\frac{V^2}{gD}\right)\left(\frac{\rho_f}{\rho_s-\rho_f}\right)\sqrt{C_D}\right]^{-3/2} \tag{11}$$

At modified Fr number less than 5, the experimental data of slurry C, D, and F match the classical correlation very well. At larger modified number (larger velocity), the flow tends to

show the homogeneous flow, and the over-pressure term decreases sharply. Note that Eq.11 is only suitable with the slurry flowing in horizontal pipe. In vertical pipe flow, the over-pressure does not appear as long as the flow velocity is larger than the fall velocity of the particles and the friction loss can be calculated as for a homogeneous suspension, employing the correct density and viscosity terms. Figure 16 shows that the larger particle size results in a smaller over-pressure term (see curve of slurry E). From an engineering application standpoint, Eq.11 could be used to predict the pressure gradient for the complicated slurry flow. At higher flow velocity, the pressure gradient can easily be calculated as homogeneous flow.

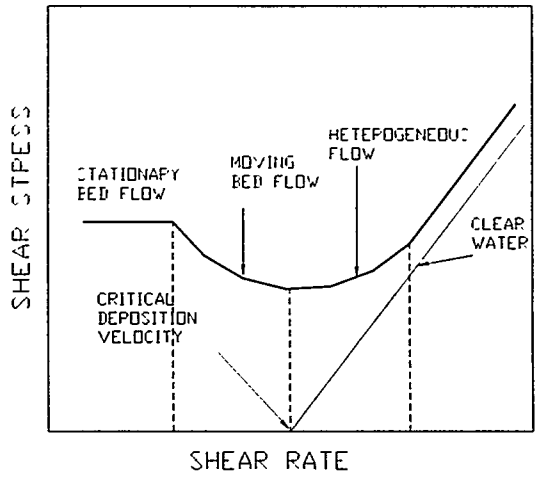

Figure 9. Typical wall shear stress versus shear rate for simple slurry.

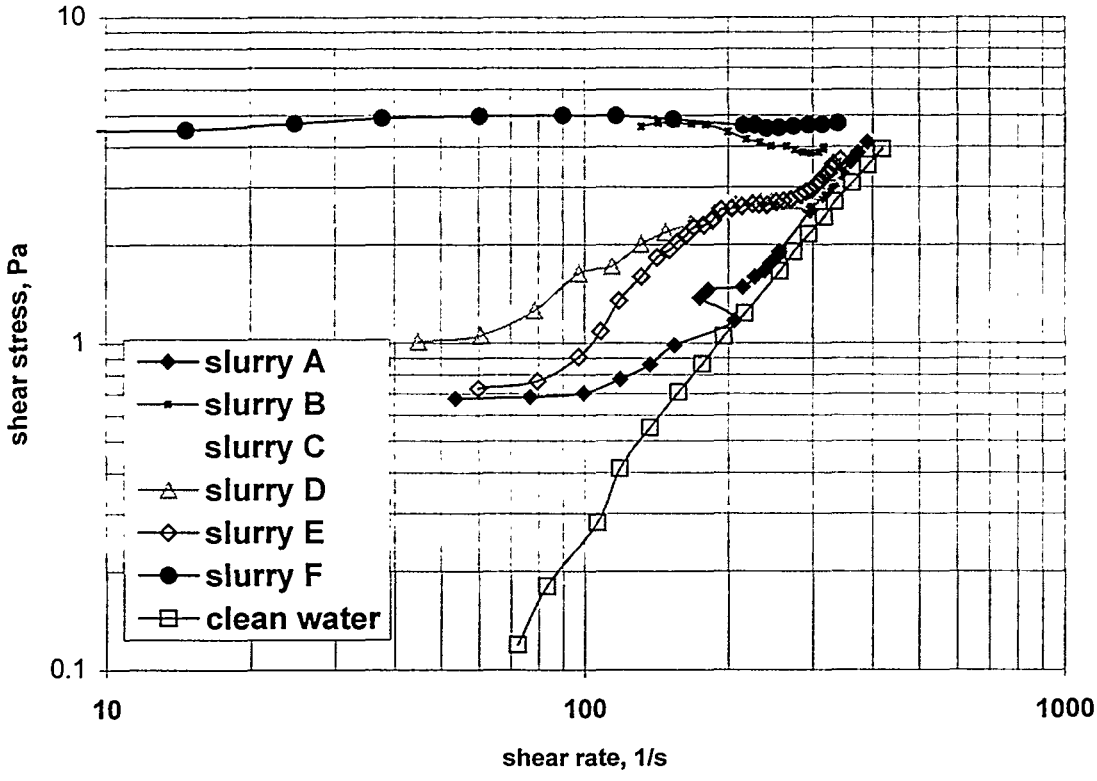

Figure 10. Wall shear stress versus shear rate for the six slurry simulants.

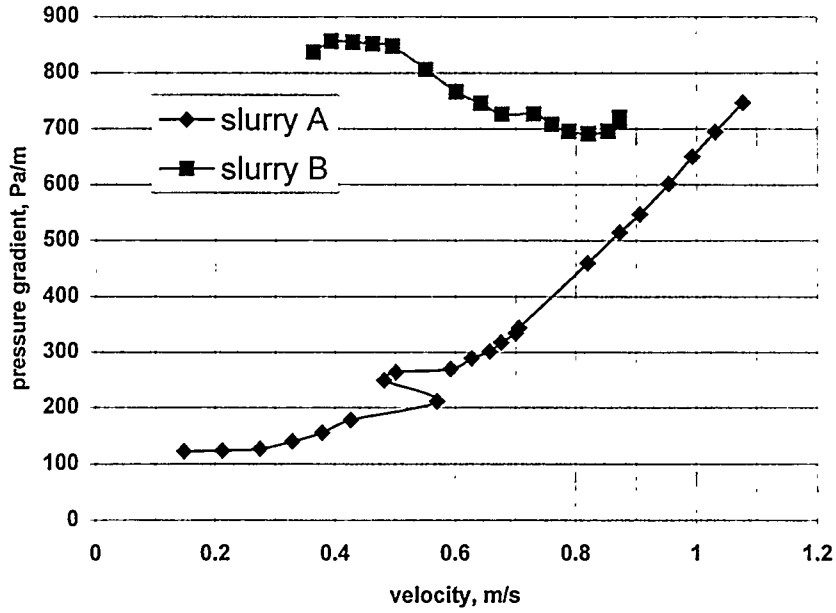

Figure 11. Pressure gradient versus flow velocity (volume concentration effect).

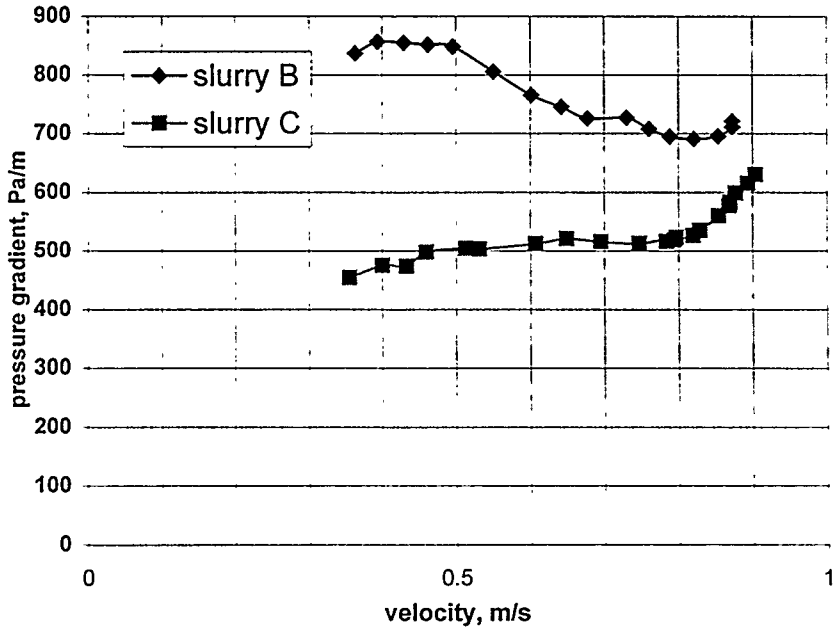

Figure 12. Pressure gradient versus flow velocity (particle size effect).

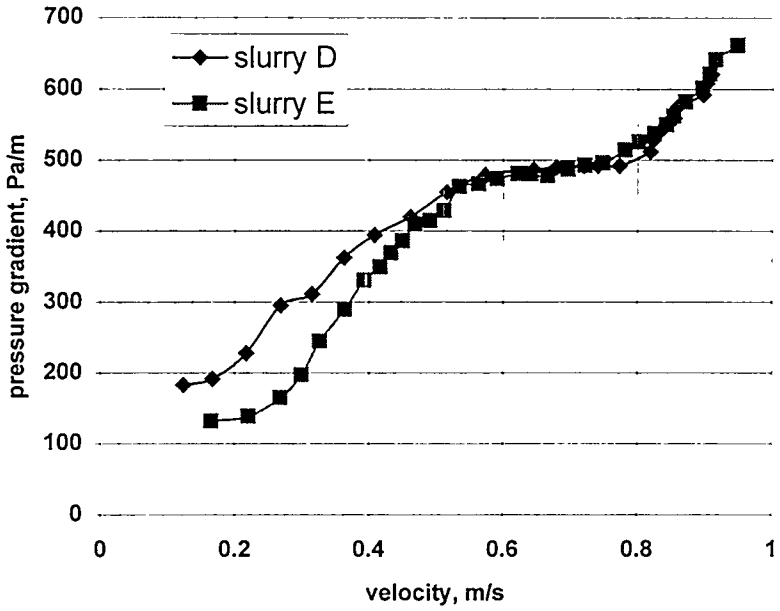

Figure 13. Pressure gradient versus flow velocity (particle size effect).

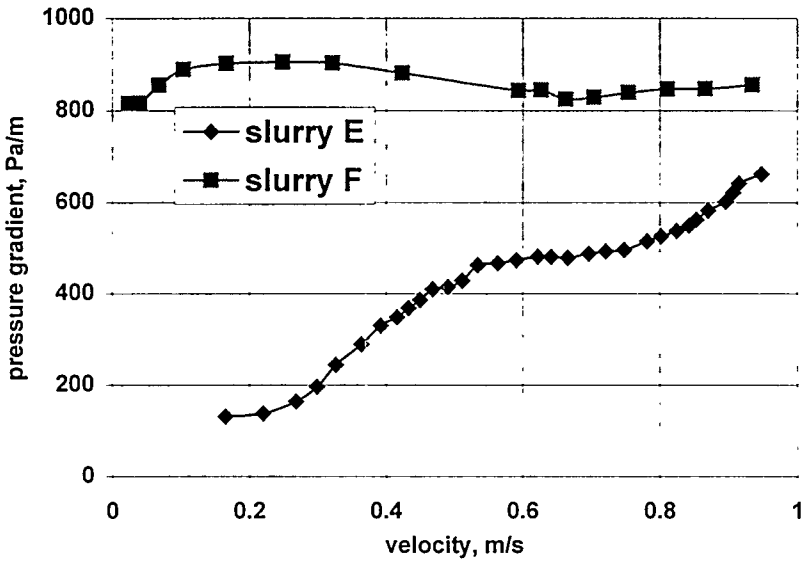

Figure 14. Pressure gradient versus flow velocity (volume concentration effect).

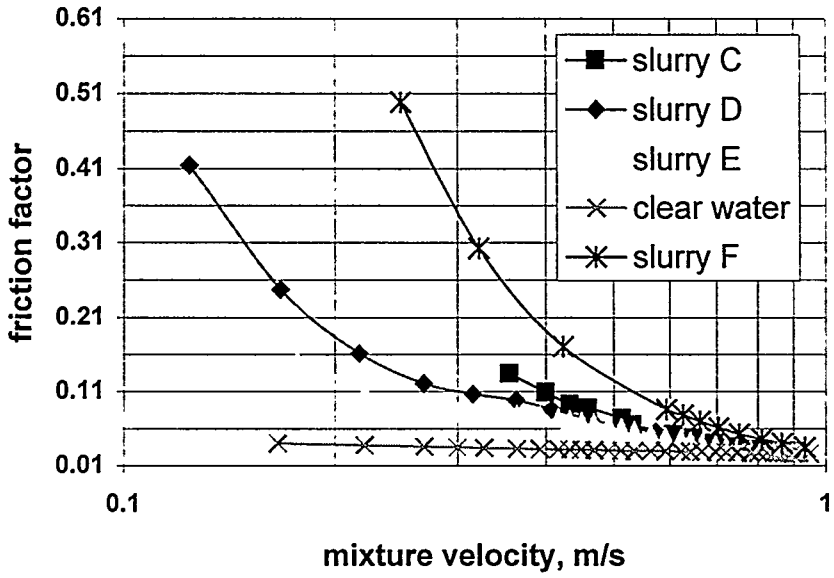

Figure 15. Friction factor versus flow velocity.

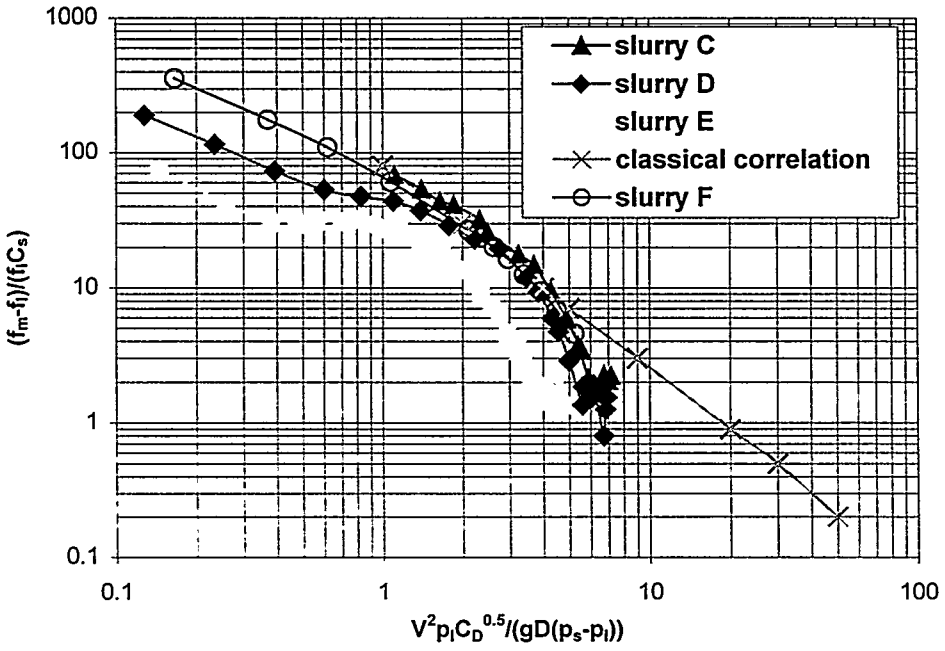

Figure 16. Over-pressure term versus modified Fr number and comparison with the classical correlation.

5.0 FLOW PATTERN AND WEIGHT CONCENTRATION DISTRIBUTION ALONG FLOW DIRECTION

In the design of a slurry transfer system, one of the main concerns is the prior knowledge of the pumping power input required. If the pump can not supply the suitable slurry mixture velocity, the settling process may occur and eventually induce the pipe plugging. In order to know at what condition the particles settle down, it is necessary to know the flow pattern of the liquid-particle two-phase flow. The slurries can be transported in one of the following flow regimes:

- Pseudo-homogeneous flow
- Heterogeneous flow
- Stationary bed flow
- Moving bed flow.

5.1 PSEUDO-HOMOGENEOUS FLOW

Homogeneous flow may occur under the condition of high slurry flow velocity, fine particle size, and low particle concentration. There is no concentration gradient across the vertical cross-section. It is also assumed that no slip between the liquid and the particles exists. All particles are suspended in the mixtures. This is a good operating condition for homogeneous flow in the pipe.

5.2 HETEROGENEOUS FLOW

For most slurry transfer conditions, the slurry shows heterogeneous flow characteristics. Because the slurry velocity is not high enough, the concentration gradient at the vertical cross-section is established. That is, due to the particle gravity, the concentration is higher in the lower part of the cross-section than it is in the upper part of the cross-section. However, all the particles are suspended in the mixture.

5.3 STATIONARY BED FLOW

At low slurry velocity, the buoyancy force and the turbulent eddy can not balance the particle gravity, causing the particle settling down. A stationary bed is formed in the low part of the pipe; the liquid—which may contain a suspension of fine particles—flows in the upper part of the pipe. On the interface of the particle bed and the liquid, some particles may settle down to the interface. But, after some time, these particles may also resuspend in the flowing mixture again. Generally, when particles are mixed with the Newtonian fluid, it is possible to form stationary a bed flow at low velocity.

5.4 MOVING BED FLOW

When the carry fluid shows non-Newtonian characteristics, a "moving bed" flow at low slurry velocity may result. However, the available literature also indicates that moving bed flow is not the true case for slurry flow; thus, a three-layer model was presented. Such a model indicates that while the upper strata of the bed may be moving, the lower strata may be stationary. (See P. Doron et al. 1993).

As mentioned in the last section, for the six typical slurry simulants investigated in this study, two main flow patterns exist with the present experiment ranges. One is the heterogeneous flow, and the other is the stationary bed flow. The transition appears at the limit deposition velocity, after which further decreasing the flow velocity will result in the stationary bed flow.

In the heterogeneous flow region, the weight concentrations at the top point and bottom point along the flow direction were measured by sucking samples from the sampling tube. The detailed sampling location is shown in Figure 1. The measurement covered the range of flow rate from 1100 L/h to 1500 L/h. The run case parameter is shown in the following table. The results for slurry C are shown in Figures 17~19.

Table 9.
Weight concentration run-case parameter

Run case	Flow rate(L/h)	ΔP1(in H_2O)	ΔP2(in H_2O)	ΔP3(in H_2O)
Case 1	1100	14.0	1.4	13.9
Case 2	1460	21.0	2.0	21.0
Case 3	1537	23.0	2.24	23.4

From these figures, the following conclusions may be drawn:

1. Generally, there is no weight concentration gradient along the axial distance within the measuring accuracy range.
2. There is always a weight concentration gradient along a vertical cross-section. The concentration is higher on the bottom part of the pipe than on the upper part of the pipe. For instance, the weight concentration difference between the bottom point and the top point is 15% with flow rate of 1100 L/h. However, the difference is decreased to 11% for 1537 L/h flow rate.
3. With slurry flow increase, the increased turbulence results in the small weight concentration gradient across the vertical direction.

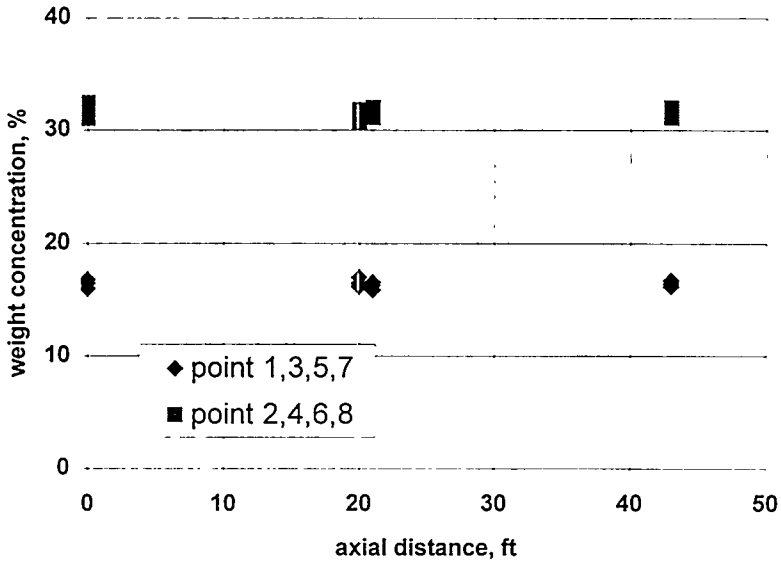

Figure 17. Weight concentration for slurry C along axial distance (case 1).

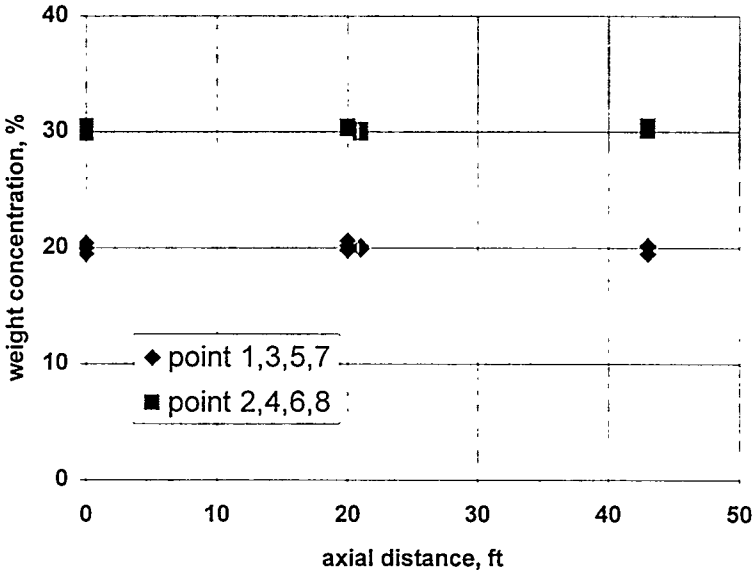

Figure 18. Weight concentration for slurry C along axial distance (case 2).

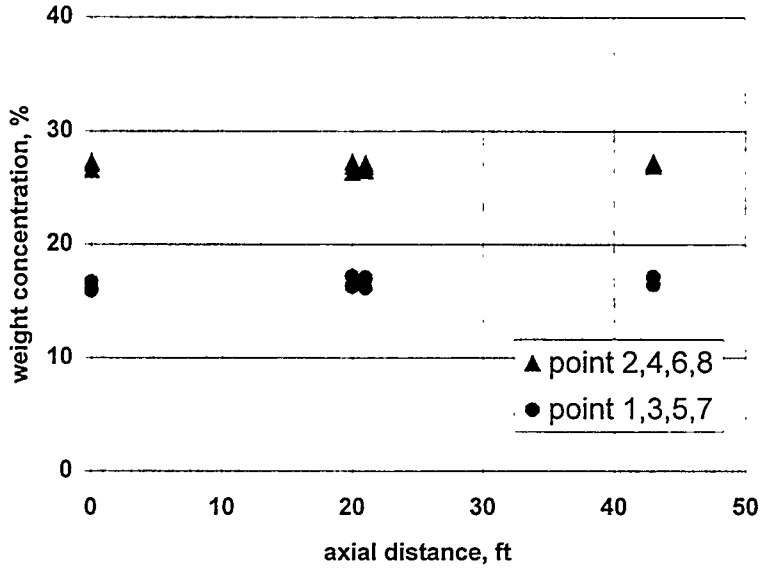

Figure 19. Weight concentration for slurry C along axial distance (case 3).

6.0 RESUSPENSION TRANSITION FOR SLURRY FLOWING IN HORIZONTAL PIPES

When more and more particles settle in the bottom of the pipe and the pipe becomes plugged, unplugging should be done to make the particles resuspend. Such a process begins with operating the slurry pump. Carefully increasing the rotating speed of the pump may result in velocity in the pipe. Typical resuspension transition for slurry A is illustrated in Figure 20 for pressure gradient and Figure 21 for flow velocity. Generally, the transition can be divided into two periods.

The first period dominated in the pipe with an elapsed time of nearly 14 minutes. The available flow area is very little, due to the plugging. The small, oscillating velocity flowed in the crack of the pipe. ΔP_1 rose sharply at the beginning of the transition, and ΔP_2 rose at nearly 7 minutes. Generally, ΔP_1 was larger than ΔP_3. The velocity is very small in the first period and just begins to rise at the end of the first period.

The second period dominated in the pipe after an elapsed time of 14 minutes. The velocity increased sharply at the beginning of this period, indicating that the available flow area increased due to the settled particle resuspension. The difference between ΔP_1 and ΔP_3 disappeared, showing that the whole horizontal pipe became resuspended at the same time, which is distinct from the first period. Following 20 minutes, the stationary bed flow was established, and the pressure gradient only got a slight variation, even though the velocity was still increasing.

Figure 20 shows that the slurry pump should overcome the pressure gradient of 900 Pa/m. The total pressure drop was estimated to be 0.28 bar (4.05 Psi) based on the total pipe length of 31 m (101.7 ft).

Figure 22 shows both the decreasing flow and increasing flow data transferred to the wall shear stress versus shear rate. The increasing flow curve shows that the shear stress oscillated at low shear rate, indicating that the resuspension transition is a time-varying transition.

Further increasing the shear rate to 260 s^{-1} will result in the intersection of the increasing flow curve and the decreasing flow curve. The flow velocity at which the two curves intersect is named as the resuspension velocity. At a flow velocity greater than the resuspension velocity, the heterogeneous flow will be established in the pipe. The resuspension velocity is very important for the engineering application, because it specifies at what velocity the solid particles become fully resuspended.

Table 10 illustrates the resuspension velocity for the six slurry simulants. Table 11 summarizes the maximum pressure gradient and the resuspension velocity for the unplugging process.

Table 10.
The resuspension velocity for the six slurry simulants

Slurry simulants	Resuspension velocity (m/s)
A	0.69
B	1.25
C	0.90
D	0.88
E	0.87
F	1.32

Table 11.
The maximum pressure gradient for the unplugging of the horizontal pipe

Slurry	Pressure gradient required for unplugging
A	900 Pa/m
B	1200 Pa/m
C	700 Pa/m
D	1400 Pa/m
E	700 Pa/m
F	2000 Pa/m

The maximum pressure gradient for slurry B with 20% weight concentration, only fine particles, is 1200 Pa/m. However, the pressure gradient is decreased to 700 Pa/m for slurry C with the same weight concentration as slurry B but with "coarse" particle size of 180~250 μm. From this can be inferred that the maximum pressure gradient for the unplugging of the pipe is larger for slurries with "finer" particles. Similar conclusions can be drawn from comparing the results between slurry D and slurry E. Slurry F with 30% weight concentration has the maximum pressure gradient.

The resuspension transition can be summarized as follows:

- The transition can be divided into two different time periods.
- In the first period, the available flow area is very small due to the pipe plugging. The slurry flows at a low velocity through the crack of the pipe. The pressure gradient increased sharply, and ΔP_1 is always larger than ΔP_3.
- In the second period, the velocity rose sharply. The pressure gradient oscillated, followed by a slight varying versus time. The stationary bed was established in this period.

- The resuspension velocity, which is very important for the engineering application, is only slightly greater than the limit deposition velocity.
- The particle size has a strong effect on the resuspension transition. Larger particle size will result in a smaller pressure gradient to unplug the horizontal pipe.

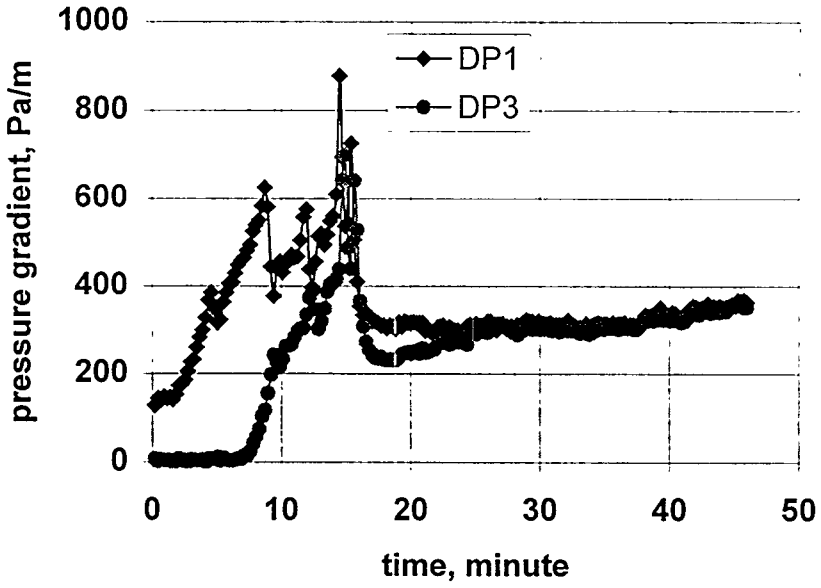

Figure 20. Pressure gradient versus time for resuspension transition with slurry A.

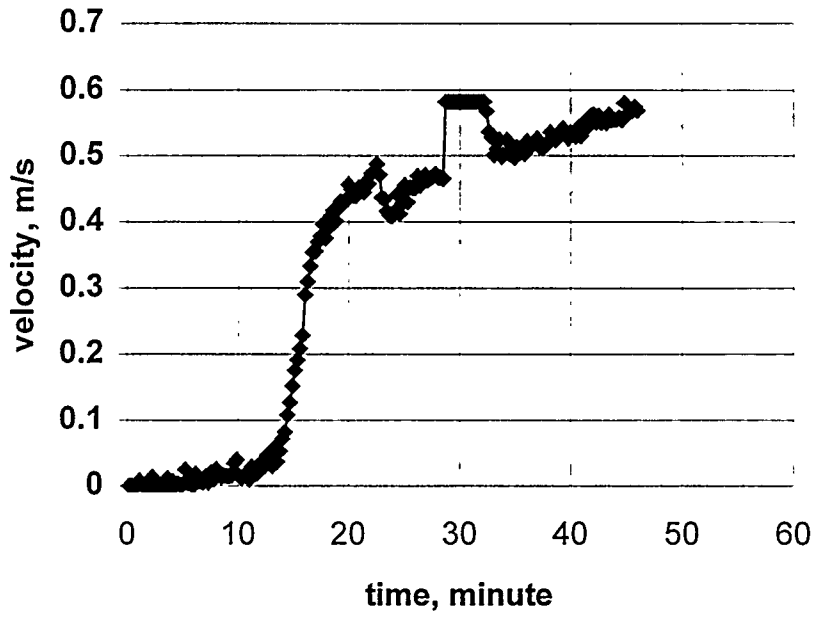

Figure 21. Flow velocity versus time for resuspension transition for slurry A.

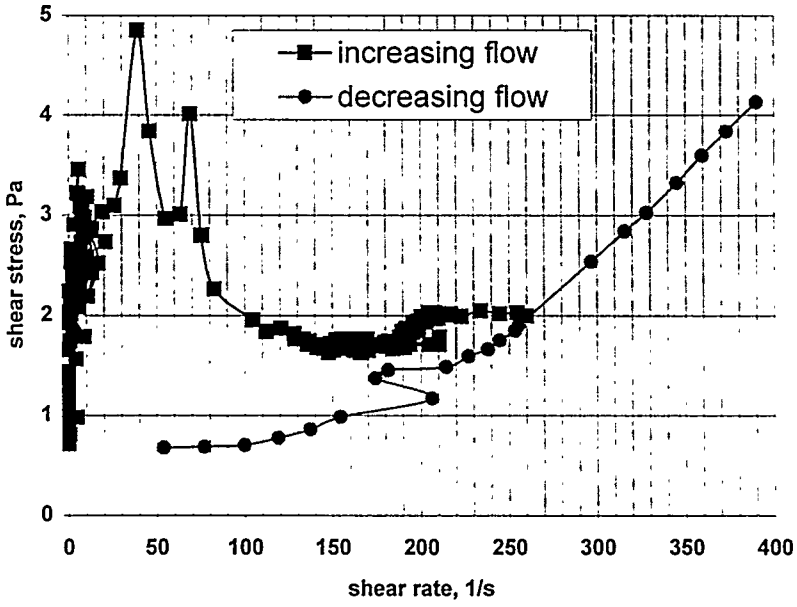

Figure 22. Shear stress versus shear rate for both increasing flow and decreasing flow.

7.0 THE DESIGN OF PIPELINE PLUGGING AND UNPLUGGING LARGE-SCALE DEMONSTRATION TEST BED

FIU-HCET will continue to investigate pipe plugging and unplugging behaviors of waste slurry transfer lines for a high-level waste (HLW) system on the waste transfer simulation flow loop in FY99. In FY98, in addition to the flow loop experimental investigation on the slurry flowing in pipelines, FIU-HCET did much preparation on the large-scale demonstration test bed. The concept design of the test bed has been finished, following two meetings with NHC and PNNL on August 24, 1998, and October 5, 1998. Based on their suggestions, the design shall be condensed to three cases from the original five pipeline design cases provided in the document "Functions and Requirements for Blockage Locating and Removal Methods in Waste Transfer Lines."

In the attached drawings, Figure 23 shows the designs for original case 1 and original case 5; Figure 24, for the original cases 2, 3, and 4. Figure 25 shows the design for the buried pipeline.

The New Design of Pipeline

Three design cases were provided, each including some elements of original cases outlined by J. Coughlin and E. Szendrei (1998). The total length was 86 ft for the first case, 3050 ft for the second, and 30 ft for the buried pipe.

In Figure 23, the pipeline includes original case 1 and original case 5elements. The design represents typical gravity drain pipelines, which include the jumper at evaporator, inclined pipe with 86 ft length and 2-inch diameter, and cleanout bottom lines with 1-inch diameter.

The reproduced case 5 (see Figure 26 for detail) uses 2-inch pipe arranged on the vertical plane. It consists of three typical curved pipe sections with curve radii of 24 and 10 inches.

Long pipes and various bend angles are the major characteristics of original case 2. In the reproduced case 2 (see Figure 24), the longest pipe (3000 ft) reflects nearly the half length of the pipe from BLDG 2 to BLDG 3. Another pipe section of 50 ft was combined with the longest pipe with a bend angle of 90°. Only the sections reflecting the major characteristics of pipeline layout from original case 2 are incorporated into the new design. In the original case 2, the bend angle varies from 28°34' to 90°. It is believed that if the unplugging method works for an angle of 90°, it should work for all other angles in between.

Figure 25 shows the buried pipe. Two pipes, one with 4-inch diameter and the other with 3-inch diameter, are buried in the concrete. Other dimensions can be seen in Figure 25.

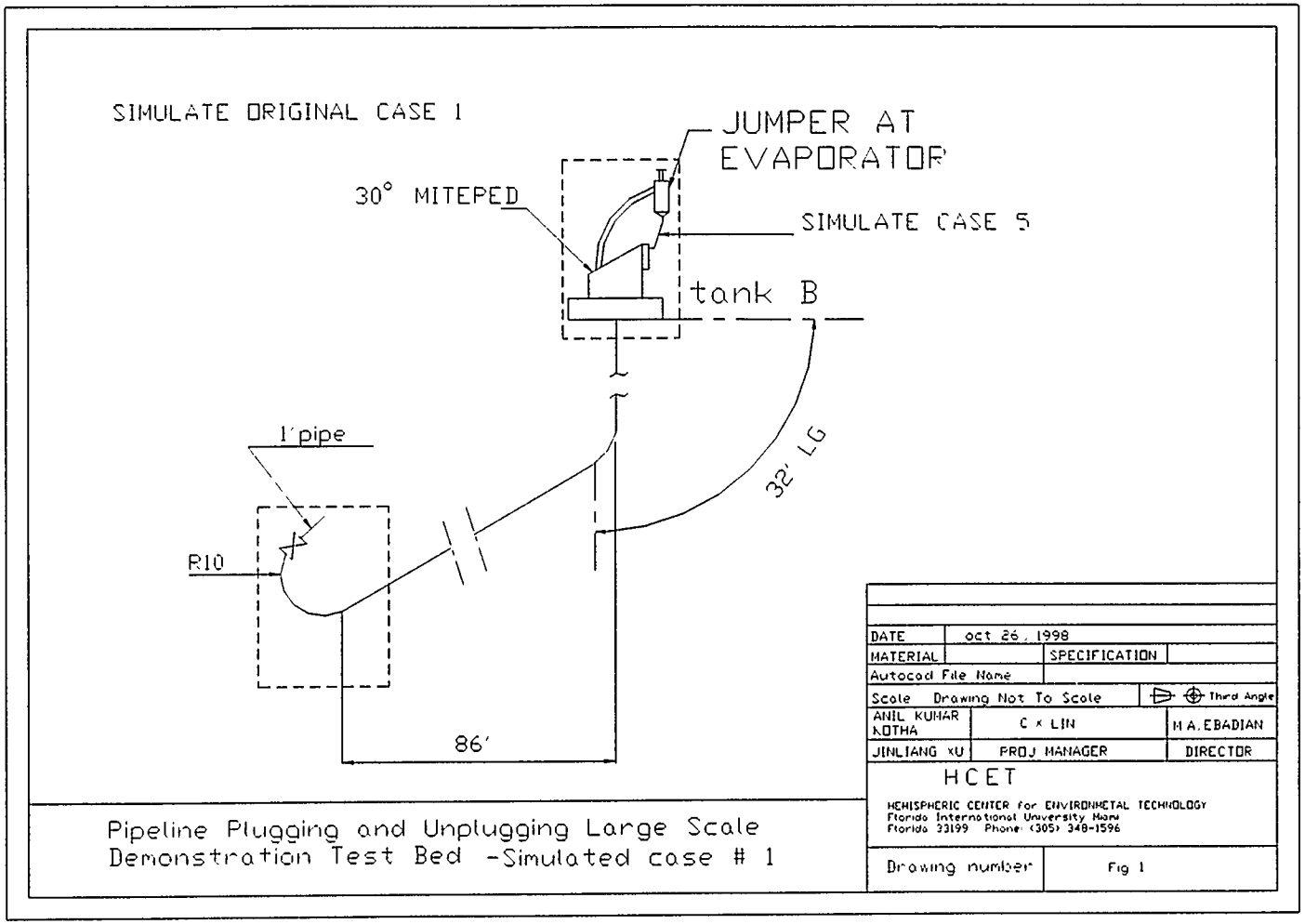

Figure 23. Pipeline plugging and unplugging large scale demonstration test bed- simulated case #1.

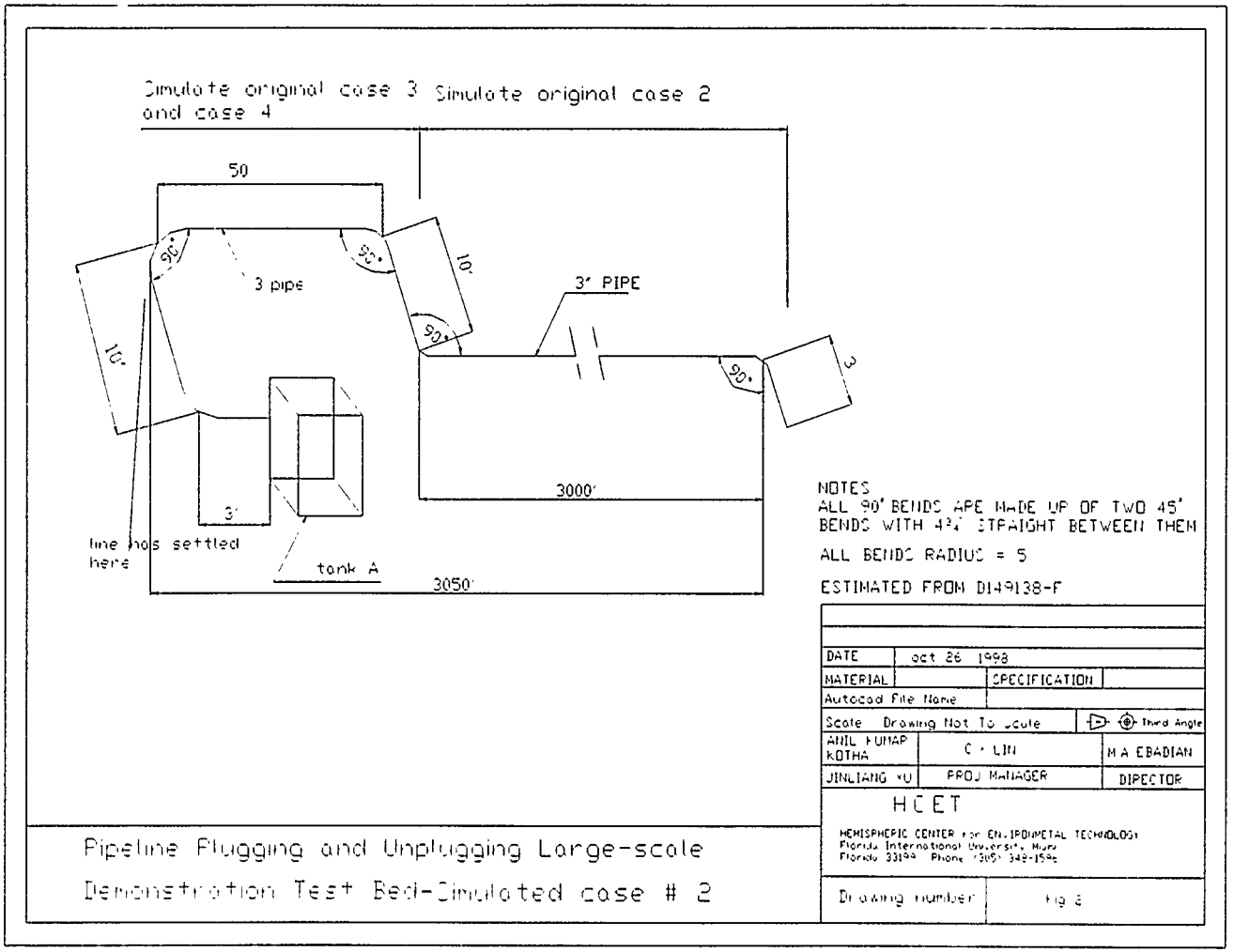

Figure 24. Pipeline plugging and unplugging large scale demonstration test bed- simulated case #2.

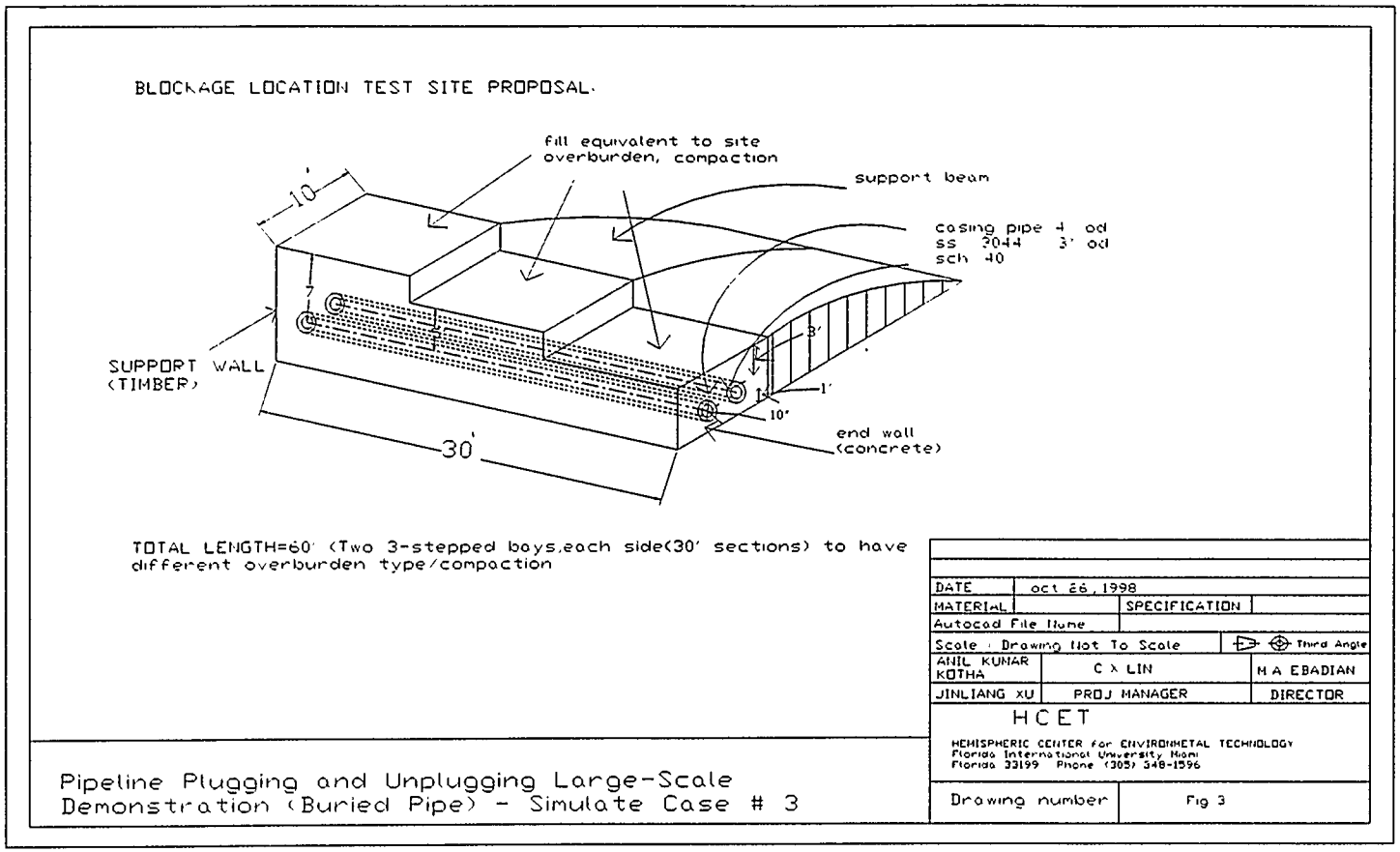

Figure 25. Pipeline plugging and unplugging large scale demonstration test bed- simulated case #3.

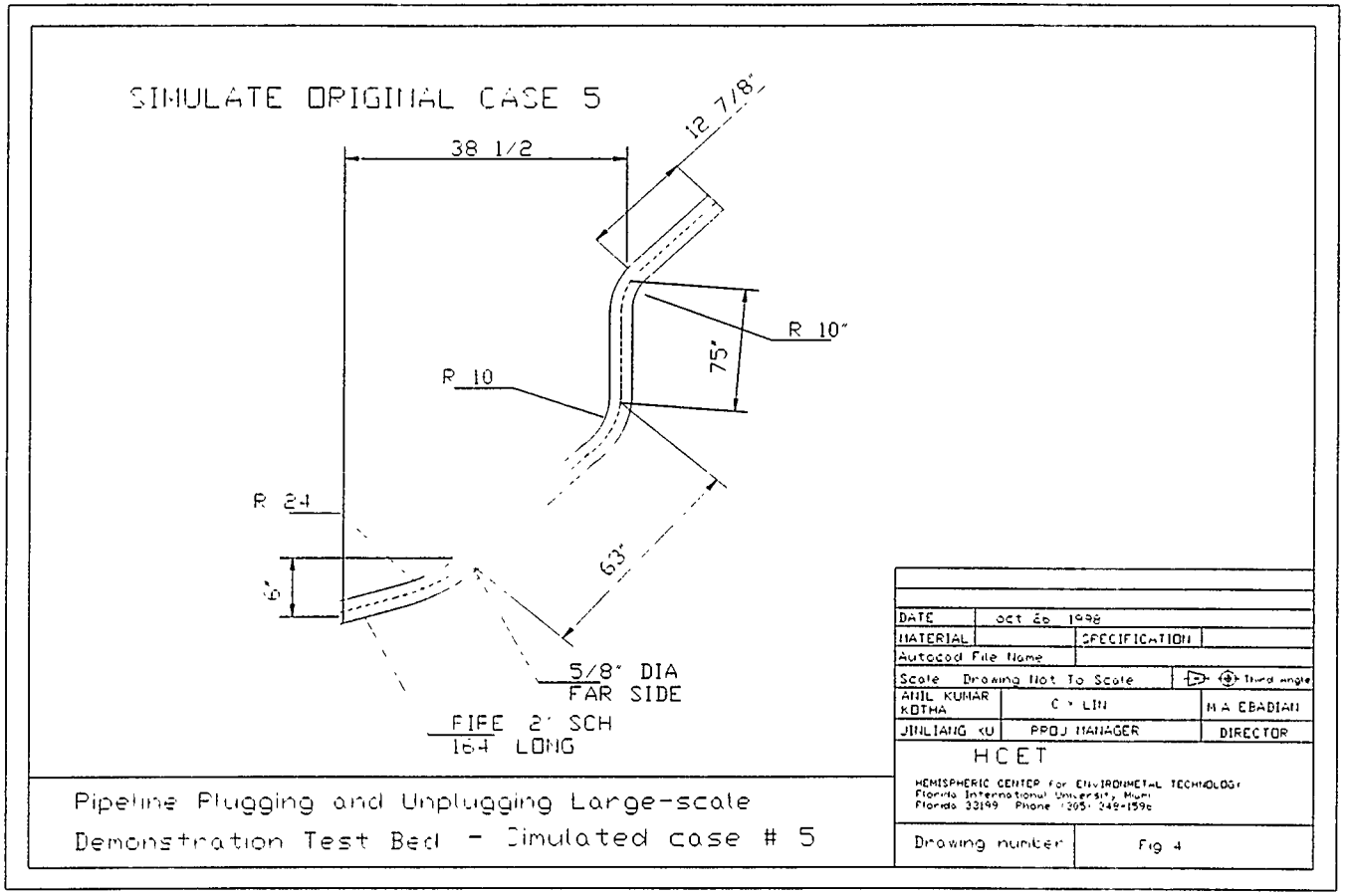

Figure 26. Pipeline plugging and unplugging large scale demonstration test bed- simulated case #5.

8.0 MAJOR ACCOMPLISHMENTS AND CONCLUSIONS

In FY98, FIU-HCET personnel have accomplished the following and reached the following conclusions:

1. A flow loop for slurry flowing in horizontal pipe and pipe with a dip has been constructed at FIU-HCET. The loop contains a mixing tank, pump, pipelines, and corresponding measurement transducers. An efficient sampling system was developed to suck the samples from the top points and the bottom points along the flow direction. The Lab-View Data Acquisition system was applied to record and store the steady or the transition data.
2. Six typical slurry simulants of interest to DOE sites were used-among them, three simulated Savannah River slurries and three simulated Hanford slurries. The physical properties were measured or calculated. The viscosities were measured by the HAKKE viscometer.
3. Preliminary data and results were provided for the six slurry simulants flowing in horizontal pipelines, with attention to the flow characteristics, settling, and pipeline plugging. Both the decreasing flow and the increasing flow tests were completed.
4. Within the present operating parameters, the flow has two different flow patterns: the heterogeneous flow and the stationary bed flow. The transition appears at the critical velocity, which is important for the engineering application to avoid the particle settling.
5. At the heterogeneous flow pattern, the weight concentration measurements from the top points and the bottom points show that there is always a weight concentration gradient across the vertical cross-section, but no gradient exists along the flow direction.
6. At stationary bed flow, further decreasing the flow velocity will result in more and more particles settling. The available flow area is decreased, and eventually the pipe is plugged.
7. A correlation was recommended to predict the pressure gradient (flow resistance). Resuspension tests were also done to unplug the horizontal pipe. It was found that two periods, showing different characteristics, existed during the whole unplugging process. The maximum pressure gradients (unplugging resistance) and the resuspension velocities for the typical slurry simulants were obtained. At the fixed particle volume concentration, the slurry simulants with fine particles will get higher unplugging resistance. At the fixed particle sizes, the larger volume concentration will get higher unplugging resistance.
8. Numerical modeling of slurry simulants flowing in horizontal pipes is in process. Grid generation has been finished; the liquid-solid two-phase model has been chosen; and the boundaries have been specified.
9. In addition to the flow loop experimental investigation of slurry flowing in pipelines, FIU-HCET prepared a large-scale demonstration test bed. The concept design of the test bed has been finished, as a result of two meetings with NHC and PNNL on August 24, 1998, and October 5, 1998. Based on their suggestions, the design is being condensed to three cases from the original five pipeline design cases.

9.0 PLANNED ACTIVITIES FOR FY99

FIU-HCET will continue to investigate pipe plugging and unplugging behaviors of waste slurry transfer lines for a high-level waste (HLW) system on the waste transfer simulation flow loop in FY99. In addition to the pipe plugging caused by settling, pipe plugging and unplugging phenomena induced by gelling will also be studied by both experimental and theoretical methods.

In FY99, activities for industrial equipment tests and demonstrations of plug locating and pipe unplugging technologies will be coordinated by FIU-HCET, NHC, PNNL, FETC, and DOE sites. FIU-HCET will complete the design and construct the Plug Locating and Removal Demonstration test bed for the industrial equipment test and demonstration to be conducted in FY00. FIU-HCET will also plan additions to the large-scale (full-size) test bed required for pipeline inspection tools testing in the future.

The major objective of this work is to further understand the pipeline plugging and unplugging mechanism by particle settling and gel formation, to identify and test industrial methods to locate and remove waste transfer pipeline blockage, and to inspect and certify the condition of those pipelines.

The following tasks will be performed to ensure that the project objectives are met and that all work is conducted according to a performance-based schedule.

Task 1 Flow Loop Research on Pipeline Plugging and Unplugging

TASK 1.1 EXPERIMENTAL INVESTIGATION OF SETTLING-CAUSED PLUGGING

The slurry settling and settling-caused pipe plugging process will continue to be investigated with the existing experimental system, which was fabricated in FY98. Important aspects to be examined include particle agglomeration due to certain physical/chemical conditions and the effects of shutting down the slurry pump. The effects of pump shutdown will be conducted with a long pipeline with a dip.

TASK 1.2 THEORETICAL STUDY OF SETTLING-CAUSED PLUGGING PROCESS

The slurry flow with settling process will continue to be investigated with a computational method. Based on previous numerical studies in FY98, the mathematical model will be modified and improved. The major work will focus on the simulation of the plug-developing process and the estimation of the plugging risk for waste slurry in pipeline transfer systems.

TASK 1.3 IDENTIFY AND PREPARE SLUDGE SIMULANTS AND LUBRICATING LIQUID FOR GELLING TESTS

Sludge simulants of similar physical and chemical properties as those at DOE sites will be used for this experimental study of gelling-caused plugging and unplugging. A chemical system must be chosen that can form gels in a reversible manner. A bench-scale test will be performed to determine if the gelling process is caused by temperature change or by chemical additives. The selected lubricant must be immiscible in the gelled sludge.

TASK 1.4 DESIGN AND MODIFY EXISTING EXPERIMENTAL SETUP FOR GELLING TESTS

The existing slurry settling experimental system will be redesigned and modified for experiments on sludge gelling, plugging, and unplugging processes. The core-annular flow technology may be incorporated in the experimental system for unplugging the gel blockage in the pipeline. The experimental setup will include a cooling section, a constant temperature section, and a lubricant liquid injection system to maintain required test conditions. A transparent section may be used to visualize the gelling process. In addition to flow rate, sludge concentration, and pressure drop, temperature and gel properties will also be monitored.

TASK 1.5 EXPERIMENTAL INVESTIGATION OF GELLING-INDUCED PLUGGING AND UNPLUGGING

This is the major part of the flow loop research activities of pipeline plugging and unplugging in FY99. The gelling-induced plugging and unplugging processes will be tested simultaneously with the experimental setup. The sludge flow characteristics, gelling process, and core-annular flow behaviors in pipelines will be investigated extensively with the experimental setup within wide parameter ranges. Major parameters to be examined in the experiments include temperature, chemical additives, flow rate, sludge concentration, and pH values.

TASK 1.6 THEORETICAL ANALYSIS OF GELLING-CAUSED PLUGGING AND UNPLUGGING PROCESSES

Computational studies will be conducted to investigate the plugging and unplugging process associated with gel formation. The core-annular flow behavior and its instability in long pipelines will be highlighted. A mathematical model will be proposed and will be validated and improved based on the experimental results.

Task 2 Large-Scale Industrial Equipment Test of Plug Locating and Unplugging Technologies

TASK 2.1 IDENTIFY AND DETERMINE COMPANIES AND THEIR POTENTIAL TECHNOLOGIES FOR EQUIPMENT TESTS AND DEMONSTRATIONS

FIU-HCET will cooperate with FETC, NHC, PNNL, DOE and its major sites to identify and determine companies and technologies to be tested and demonstrated at the plugging and unplugging test bed at FIU-HCET. Companies to be selected must have either plug locating or pipe unplugging technologies or both. This activity will be based on the Call for pipeline unplugging and blockage detection equipment testing to be issued by FETC.

TASK 2.2 DESIGN OF THE TEST BED FOR EQUIPMENT TESTS AND DEMONSTRATIONS

A test bed of full size will be designed at FIU-HCET for the industrial equipment tests and demonstrations. For the most part, unburied pipes with plugs will be tested. Depending on the nature of plug locating and unplugging technologies, buried pipes with plugs may also be tested. In the test bed, both gravity pipeline and long pipeline will be set up. The plug or blockage will be prepared by FIU-HCET. A monitoring system to ensure the tested technology has really located and unplugged the blocked pipeline will be developed.

TASK 2.2 CONSTRUCTION OF THE TEST BED FOR EQUIPMENT TESTS AND DEMONSTRATIONS

After the design is finalized, the large-scale test bed will be fabricated at FIU-HCET for the industrial equipment tests and demonstrations of plug locating and unplugging technologies.

FIU-HCET plans to conduct the large-scale pipeline plug locating and removing equipment test and demonstration in FY00.

Task 3 Pipeline Inspection Tools

TASK 3.1 PLAN ADDITIONS TO FULL-SIZE TEST BED FOR PIPELINE INSPECTION

In FY99, FIU-HCET will collaborate with NHC, PNNL, FETC, DOE and its sites for preparation of the activities associated with pipeline inspection tools. Based on the Functions and Requirements for pipeline inspection issued by SRS, FIU-HCET will provide test bed modification plans for pipeline inspection tool testing.

FIU-HCET plans to conduct pipeline inspection testing of FETC-sponsored industrial methods in FY01.

10.0 REFERENCES

Brown, N.I., and Heywood, N.I., 1991, *Slurry Handling: Design of Solid-Liquid Systems*. Elsevier Science Publishers, London.

Charles, M.E., and Charles, R.A., 1971, The use of heavy media in the pipeline transport of particulate solids. In *Advances in Solid-Liquid Flow in Pipes and Its Applications*, ed. I. Zandi. Pergamon Press, Oxford, UK, 187-197.

Coughlin, J., and Szendrei, E., 1998, *Functions and Requirements for Blockiage Locating and Removal Methods in Wast Transfer Lines*

Doron, P. et al. 1993 A Three-Layer Model for Solid-Liquid Flow in Horizontal Pipes, *Int. J. Multiphase Flow.*

Durand, R., and Condolios, E., 1952, Experimental study of the hydraulic transport of coal and solid materials in pipes. Proc. Colloq. On the Hydraulic transport of Coal, National Board, UK, 39-55.

Fangary, Y.S. et al. 1997 Minerals, Engineering, the Effect of Fine Particles on Slurry Transport Process

Gillies, R.G., Shook, C.A., and Wilson, K.C., 1991, An improved two-layer model for horizontal slurry pipeline flow. *Can. J. Chem. Eng.*, 69, 173-178.

Hisamitsu, N., Shoji, Y., and Kswugi, S., 1978, Effect of added fine particles on flow properties of settling slurries. *Hydrotransport 5, BHRA Fluid Engineering*, Cranfield, Bedford, England, 29-49.

Hou, H.C., 1986, Investigation of optimal grain distribution for transport with high concentration. *Hydrotransport 10, BHRA Fluid Engineering*, Cranfield, Bedford, England, 177-183.

Hou, H.C., 1988, On the optimal concentration of fine particles in hydrotransport. *Hydrotransport 11, BHRA Fluid Engineering*, Cranfield, Bedford, England, 285-294.

Jacobs, B.E.A., 1990, *Design of Slurry Transport Systems*. Elsevier Applied Science, London.

Kenchnington, J.M., 1976, Prediction of critical conditions for pipelines flow of settling particles in a heavy medium. *Hydrotransport 4, BHRA Fluid Engineering*, Cranfield, Bedford, England, 31-48

Newitt, D.M., Richardson, J.F., Abbott, M., and Turtle, R.B., 1995, Hydraulic conveying of solids in horizontal pipes. *Trans. Instn. Chem. Engrs.*, 33, 93-113.

Sakamoto, M., Mase, M., Nagawa, Y., Uchida, K., and Kamino, Y., 1978, A hydraulic transport study of coarse materials including fine particles with hydrohoist. *Hydrotransport 5, BHRA Fluid Engineering*, Cranfield, Bedford, England, 79-80.

Shook, C.A., and Roco, M.C., 1991, Slurry Flow Principles and Practice. Butterwoth-Heinemann, Boston.

Wasp, E.J., 1978, Solid-Liquid Flow, Slurry Pipeline Transportation

Wilson, K.C., Clift, R., Addie, G..R., and Maffett, J., 1990, Effect of broad particle grading on slurry stratification ratio and scale-up. *Powder Technol.*, 61, 165-172.